

Nucleon-Nucleon interactions from effective field theory

José A. Oller^{#1}

*Departamento de Física. Universidad de Murcia.
E-30071, Murcia. Spain.*

Abstract

We have established a new convergent scheme to treat analytically nucleon-nucleon interactions from a chiral effective field theory. The Kaplan-Savage-Wise (KSW) amplitudes are resummed to fulfill the unitarity or right hand cut to all orders below pion production threshold. This is achieved by matching order by order in the KSW power counting the general expression of a partial wave with resummed unitarity cut, with the inverses of the KSW amplitudes. As a result, a new convergent and systematic KSW expansion is derived for an on-shell interacting kernel \mathcal{R} in terms of which the partial waves are computed. The agreement with data for the S-waves is fairly good up to laboratory energies around 350 MeV and clearly improves and reestablishes the phenomenological success of the KSW amplitudes when treated within this scheme.

arXiv:nucl-th/0207086v2 16 Apr 2003

^{#1}email: oller@um.es

1 Introduction

Effective field theories are the standard method to deal with strong interactions in the non-perturbative regime. As paradigm we have SU(2) Chiral Perturbation Theory (CHPT) for pion physics [1, 2, 3], where a convergent power counting is established in terms of derivatives, insertions of quark mass matrix and external sources. This has also been applied to pion-nucleon interactions with baryon number, B , equal to 1 [4]. Its extension to nucleon-nucleon physics [5, 6, 7, 8, 9, 10] is not straightforward due to the appearance of two new scales: the large scattering lengths of the S-waves and the large nucleon mass, M . The latter can be easily handled for $B=1$ although this is no longer the case for $B > 1$ [5]. Large efforts have been devoted during the last years to end with a convergent effective field theory (EFT) for nucleon-nucleon interactions including pions, for a review see e.g. [11]. On the one hand, we have the original Weinberg's proposal [5], with an undoubted phenomenological success [12]. In this scheme, the nucleon-nucleon potential is calculated in a chiral expansion up to some definite order and then the Lippmann-Schwinger equations in partial waves are solved to determine *numerically* the physical amplitudes. Nevertheless, this approach suffers from inconsistencies in the power counting due to the appearance of divergences that are enhanced by powers of the large nucleon mass. As a result, their coefficients are much larger than those expected from 'naive power counting'. Despite this, such divergences are finally reabsorbed by counterterms whose chiral orders are established by assuming natural size following dimensional arguments. On the other hand, we have the Kaplan-Savage-Wise (KSW) effective field theory [13] with its consistent power counting that directly applies to the physical amplitudes, like in standard CHPT [1, 2, 3], and one finally has *analytical* nucleon-nucleon amplitudes. Interestingly, in the KSW power counting all the ultraviolet divergences appearing in loops are canceled by contact operators appearing at either the same or lower order in the expansion. This is not the case in the Weinberg's approach where one has cut-off dependence which gives an estimate of the size of higher order corrections. However, the convergence and the phenomenological success of the KSW effective theory is just restricted to a very narrow region close to the nucleon-nucleon threshold despite having included explicitly the pion fields [14, 15]. This was clear from the analysis at NNLO in the KSW effective field theory performed in ref.[14] where the NNLO departs from data before the NLO and badly diverges for center-of-mass three-momentum above ~ 100 MeV. The reason for this bad convergence properties is the large contributions from the twice iterated pion exchange in the triplet channels. That is, pions cannot be treated perturbatively in all the nucleon-nucleon channels and in particular in the $S_1^3 - D_1^3$ one.

Hence, despite all the efforts made during the past years, the issue of deriving a consistent effective field theory for nucleon-nucleon interactions is still open. We perform in this paper a step forward by extending the range of convergence of the KSW amplitudes. In ref. [5] Weinberg proposed to calculate the nucleon-nucleon potential in a chiral expansion and then solve a Lippmann-Schwinger equation in order to treat properly the large enhancements, due to factors $2M/p$, from the reducible two nucleon diagrams which do not enter in the calculation of the potential, see also ref.[8]. From a S-matrix point of view the aim of the Weinberg's proposal can be recast so that one should resum the unitarity or right-hand cut, which is the responsible for all the unitarity bubbles with their large $2M/p$ factors. Nevertheless, solving a Lippmann-Schwinger equation is not the only way to accomplish this [16] and another one, more appropriate for quantum field theory can be established. In this way, one avoids the non trivial problems associated

with the renormalization of a Lippmann-Schwinger equation with highly singular potentials at the origin as those coming from present effective field theories.

We propose here a general scheme to resum the unitarity cut. This scheme, originally motivated as an application of the N/D method [17, 18], was already employed in meson-meson [18, 19] and meson-baryon [20, 21] systems. This method should not be confused with Padé resummations like those performed in the meson-meson or meson-baryon sectors [22].^{#2} Nevertheless, there are specific facts in the nucleon-nucleon scattering, associated with the largeness of the scattering lengths in the S-waves, that require a special treatment not present in any meson-meson or meson-nucleon system, as we explain below. In fact, a very reassuring feature of nucleon-nucleon physics is that non-perturbative effects manifests at very low center of mass three-momentum, p , as indicated by the presence of bound states and poles in unphysical sheets just below threshold. Hence, one has at his disposal the three-momentum p as a small parameter and this is of course at the basis of the old Effective Range Expansions (ERE)[23]. It is also worth stressing that all the formalism presented here is analytic.

The paper is organized as follows. In sec.2 the novel formalism contained in this work is settled. This follows the KSW power counting and the reader unfamiliar with such power counting is referred to the original literature, refs.[13, 14]. It is shown how the unitarity cut can be easily resummed in terms of a dispersion relation of the inverse of a partial wave amplitude. As a result an interacting kernel \mathcal{R} arises that is determined by matching with the pure KSW amplitudes following the KSW power counting. Once this is done, we discuss in sec.3 the phenomenology and compare with data. Since all the expressions are analytic, we fix, order by order in the expansion, many of the counterterms in terms of the ERE parameters a_s and r_0 in the S-waves. The agreement with data for the S-waves and the mixing angle $S_1^3 - D_1^3$ is quite remarkable in a broad energy range, $p \lesssim 400$ MeV ($T_{lab} \lesssim 350$ MeV), involving all the data points of the Nijmegen partial wave analysis [24]. Higher partial waves are also analyzed at the same order. However, only one pion exchange and the reducible part of twice iterated one pion exchange enter in these KSW amplitudes up to order p . The results indicate that higher order corrections should be included so as to perform a more complete analysis for the P and D partial waves, as in the Weinberg's scheme [12]. We end with some conclusions.

2 Formalism

It seems that pions cannot be treated perturbatively. This is indeed the main reason for the failure of convergence of the KSW scheme, which considers pions perturbatively in the physical amplitudes, for center of mass three-momentum $p \gtrsim 100$ MeV. This was clearly established in ref.[14], as one can see when comparing the calculated mixing parameter ϵ_1 at NLO [13] and NNLO [14]. While for very low momentum the NNLO calculations agree better with data, unfortunately for momenta higher than 100 MeV the NNLO calculations badly diverge from experiment, much more than the NLO results, and no improvement is obtained despite pions being explicitly included. This should be compared with the phenomenological success of the Weinberg's scheme in [6] and particularly in [12], where the chiral expansion seems to be under control, at least at the level

^{#2}Later one we will show that these Padé resummations are particular cases of our formalism.

of the phenomenology. In the latter scheme there are still the issues of avoiding cut-off dependence and the associated inconsistencies in the Weinberg's power counting, already referred in the introduction and originally established in refs.[8, 13].

In this paper we make use of the KSW amplitudes which are calculated within an effective field theory and are properly renormalized. There is nonetheless a clear difference between the KSW effective field theory and CHPT. While the latter is convergent in the SU(2) sector in an energy window that could be expected from the scales that are involved in the problem,^{#3} the same does not occur with the former [14].

We want to include pions non-perturbatively but keeping at the same time the advantages of the KSW scheme that make it a true effective field theory. In order to accomplish this, we resum the right hand cut or unitarity cut so as to take care of the large $2M/p$ factors from the two nucleon reducible diagrams [5]. This is also performed when solving a Lippmann-Schwinger equation, as originally proposed in ref.[5], but we will do it in a different fashion considering unitarity and analyticity in the form of a dispersion relation of the inverse of a partial wave.

Let us denote a partial wave by $T_{L_J^{2S+1}, \hat{L}_J^{2S+1}}$, where L and \hat{L} refer to the orbital angular momentum of the initial and final state respectively, and S and J indicate the total spin and total angular momentum of the systems, in order. Then unitarity requires above the nucleon-nucleon threshold and below the $NN\pi$ one, which is around $p \simeq 280$ MeV:

$$\text{Im}T_{L_J^{2S+1}, \hat{L}_J^{2S+1}} = \frac{Mp}{4\pi} \sum_{\ell} T_{L_J^{2S+1}, \ell_J^{2S+1}} (T_{\ell_J^{2S+1}, \hat{L}_J^{2S+1}})^* , \quad (2.1)$$

where M is the nucleon mass. It is easy to derive from the previous equation:

$$\text{Im} (T^{(2S+1)J})_{ij}^{-1} = -\frac{Mp}{4\pi} \delta_{ij} , \quad (2.2)$$

where $T^{(2S+1)J}$ is a matrix whose matrix elements are those triplet partial waves that mix each other, e.g. for $S_1^3 - D_1^3$ one has $T_{11}^{31} = T_{S_1^3, S_1^3}$, $T_{12}^{31} = T_{21}^{31} = T_{S_1^3, D_1^3}$ and $T_{22}^{31} = T_{D_1^3, D_1^3}$. In the previous equation we denote by $(T^{(2S+1)J})^{-1}$ the inverse of the $T^{(2S+1)J}$ matrix. If the partial waves do not mix then $T^{(2S+1)J}$ is just a number equal to $T_{L_J^{2S+1}, \hat{L}_J^{2S+1}}$. The imaginary part in eq.(2.2) is responsible for the unitarity cut. Thinking of a dispersion relation for the inverse of the amplitude this cut can be easily taken into account from eq.(2.2), as we previously did in the meson-meson [18] and meson-baryon [20, 21] sectors, and gives rise to the integral:

$$g_i(s) = \frac{1}{\pi} \int_{4M^2}^{\infty} \frac{Mp(s')}{4\pi} \frac{1}{s' - s + i0^+} ds' , \quad (2.3)$$

where s is the usual Mandelstam variable. This integral is divergent and requires a subtraction, $M\nu_i/4\pi$:

$$g_i(s) = \frac{M}{4\pi} \left(\nu_i + ip + \frac{M\sigma(s)}{\pi} \log \frac{1 - \sigma(s)}{1 + \sigma(s)} \right) , \quad (2.4)$$

with $\sigma(s) = \sqrt{1 - \frac{4M^2}{s}}$. The logarithm is purely real in the physical region and just gives rise to relativistic corrections. These are obtained from eq.(2.3) but with $Mp(s')/4\pi$ replaced by

^{#3}Except in the scalar isoscalar channel.

the relativistic phase space $M^2 p(s')/2\pi\sqrt{s}$ in the integrand. Since we want to match with the KSW amplitudes, that absorb all the relativistic corrections in the vertices, the non-relativistic phase space factor $Mp/4\pi$ is used as explicit source of imaginary part in eq.(2.4). The relativistic corrections from the logarithm of eq.(2.4) are in any case essentially negligible in the energy range that we consider. Once the unitarity cut is taken into account by the functions $g_i(s)$, the full partial wave matrix or number $T^{(2S+1)J}$ can be written as:

$$T^{(2S+1)J} = - [\mathcal{R}^{-1} + g]^{-1} . \quad (2.5)$$

In this expression all the other possible cuts of a nucleon-nucleon partial wave, either due to the exchange of other particles (in our case we have the exchanges of pions) or because its helicity structure, are included in the interacting kernel \mathcal{R} that we still must fix. The unitarity requirements, resummation of the infinite set of reducible diagrams with two intermediate nucleons, are accomplished by $g(s)$, which as stated is a diagonal matrix in the case of mixed partial waves, or just one function for the unmixed ones. For example, in the coupled partial waves S_1^3 and D_1^3 , $g_{11}(s) = g_1(s)$ and corresponds to the S_1^3 channel and $g_{22}(s) = g_2(s)$ and refers to the D_1^3 channel. Of course, $g_{12}(s) = g_{21}(s) = 0$.

We now specify \mathcal{R} in the key expression eq.(2.5). For that purpose we make use of the results of the KSW effective field theory for two nucleon systems and of its power counting, that we apply to \mathcal{R} and $g(s)$ in eq.(2.5). The matching procedure with the KSW amplitudes can be done for any given order in the calculation of the KSW amplitudes and for any subtraction constants ν_i in $g_i(s)$, as we show explicitly below.

An important point is to establish the chiral order of $g_i(s)$. This is a trivial task for the phase space and the logarithmic term in $g(s)$, eq.(2.4), since they can be expanded as a series in powers of p starting at first order. The only point we have to consider separately is the chiral order of ν_i . For the S-waves S_0^1 and S_1^3 , the corresponding elastic KSW amplitudes start at order p^{-1} and hence their inverses begin at order p . Thus one can take ν_i as order p as well, since this is the first order that appear in the inverses of the leading KSW partial waves. Would this be the case, then \mathcal{R} would also start at order p and the matching with KSW amplitudes can be performed straightforwardly. However, if we continue along these lines there is no clear improvement with respect to the problematic of the KSW calculations at NNLO. If, on the other hand, we think of higher partial waves, e.g. P and D , then we realize that the KSW amplitudes start at order p^0 so that taking g and \mathcal{R} to start as order p^0 is quite natural. If we take this option as well for the S-waves, and systematically derive the \mathcal{R} matrix elements by matching with the KSW inverse amplitudes, we will see below that the improvement with respect to the pure KSW scheme is fairly remarkable. Indeed, in order to match with the inverses of the KSW S-wave amplitudes, that start at order p , we must cancel exactly the order p^0 contributions in eq.(2.5) stemming from the ones of \mathcal{R} and g . This fine tuning reminds of the one usually advocated to explain the large scattering lengths in the S-waves channels [5].

In order to clarify further the previous discussion, we can easily see that considering ν_i as a constant of order p^0 is a result when $g(s)$ is calculated with a finite cut-off. Let us perform this illustrative exercise of more than academic importance since the finite three-momentum cut-off is the regularization employed in the Weinberg's scheme. For a given nucleon-nucleon channel i , we

Q MeV	ν MeV	Q MeV	ν MeV	Q MeV	ν MeV
100	64	500	310	900	510
200	130	600	360	1000	550
300	190	700	410	1100	600
400	250	800	460	1300	670

Table 1: Values for ν_i from eq.(2.10) for different values of the three-momentum cut-off Q .

can write:

$$g_i^c(s) = -i4M^2 \int \frac{d^4q}{(2\pi)^4} \frac{1}{(q^2 - M^2 + i0^+)((P - q)^2 - M^2 + i0^+)}, \quad (2.6)$$

where P is the total four momentum of the two nucleon system, $P^2 = s$, and the superscript c in $g^c(s)_i$ indicates that is calculated with a three-momentum cut-off. After performing the q^0 integration we have:

$$g_i^c(s) = \frac{M^2}{2\pi^2} \int_M^\Lambda \frac{\sqrt{w^2 - M^2}}{w^2 - s/4 - i0^+} dw, \quad (2.7)$$

where $\Lambda = \sqrt{Q^2 + M^2}$ with Q the three-momentum cut-off. Finally we obtain the explicit result:

$$g_i^c(s) = \frac{M^2}{4\pi^2} \left(2 \log \frac{\Lambda + Q}{M} + \sigma(s) \left[\log \frac{\sigma(s) - \frac{2M^2 + \Lambda\sqrt{s}}{Q\sqrt{s}}}{\sigma(s) + \frac{2M^2 - \Lambda\sqrt{s}}{Q\sqrt{s}}} + \log \frac{2\Lambda - \sqrt{s}}{2\Lambda + \sqrt{s}} \right] \right). \quad (2.8)$$

Performing a non-relativistic expansion in the previous equation we have:

$$g_i^c(s) = \frac{M^2}{4\pi^2} \left(2 \log \frac{\Lambda + Q}{M} + i \frac{\pi p}{M} + \sigma(s) \log \frac{1 - \sigma(s)}{1 + \sigma(s)} + \mathcal{O}\left(\frac{p^2}{M^2}\right) \right). \quad (2.9)$$

Comparing with $g_i(s)$, eq.(2.4), we finally have:

$$\nu_i = \frac{2M}{\pi} \log \frac{\Lambda + Q}{M}, \quad (2.10)$$

which is a quantity of order p^0 in the KSW power counting [13, 14]. In the KSW EFT Q is expected to be around 300 MeV, [13]. In table 1 we show the values of ν_i in MeV from eq.(2.10) for different values of Q . We will obtain later, directly from fits to data, similar values of ν_i .

Before applying the previous scheme to the KSW amplitudes, let us consider the pedagogical example of the expansion in powers of x of $f(x) = \cot x = \cos x / \sin x$. For that we write:

$$f(x) = -\frac{1}{\tau(x)^{-1} + \theta(x)}, \quad (2.11)$$

such that $\tau(x) = t_0 + t_1x + t_2x^2 + \mathcal{O}(x^3)$ and $\theta(x) = z_0 + z_1x + z_2x^2 + \mathcal{O}(x^3)$. We see here that although $f(x)$ starts at order x^{-1} we have considered the functions τ and θ to start at order x^0 . In order to fix t_i in terms of the z_i (which are assumed to be known) and of the known expansion of $\cot x$, is simpler to expand the inverse of $f(x)$, then we obtain up to $\mathcal{O}(x^2)$:

$$\frac{\sin x}{\cos x} = x + \mathcal{O}(x^3) = -\frac{1}{t_0} + \frac{t_1}{t_0^2}x + \frac{t_2}{t_0^2}x^2 - \frac{t_1^2}{t_0^3}x^2 - z_0 - z_1x - z_2x^2 + \mathcal{O}(x^3). \quad (2.12)$$

It follows then:

$$\begin{aligned} t_0 &= -\frac{1}{z_0} \\ t_1 &= \frac{(z_1 + 1)}{z_0^2} \\ t_2 &= \frac{z_2}{z_0^2} + \frac{(z_1 + 1)^2}{z_0^3}. \end{aligned} \quad (2.13)$$

It is obvious how to proceed for higher orders. This simple example also illustrates that if we want to calculate $\tau(x)$ up to order x^i one needs to know $f(x)$ up to order x^{i-2} since $f(x)$ already starts at order x^{-1} .

Let us now analyze carefully the elastic S_0^1 channel following the previous scheme. After that we will present more briefly the analogous procedure in the $S_1^3 - D_1^3$ coupled channel sector and for the P , D , F_2^2 and G_3^3 waves.

2.1 S_0^1 elastic partial wave

The KSW S_0^1 partial wave, $A_{S_0^1}^{KSW}$, was calculated at NLO (order p^0) in ref.[13] and then at NNLO (order p) in ref.[14]. Let us denote these partial waves by $A_{-1}(p)$, $A_0(p)$ and $A_1(p)$, where the subscript indicates the KSW order. As in the simple example of the $\cot x$, if we take as input the KSW amplitudes up to order p then we will be able to calculate \mathcal{R} up to order p^3 . This unambiguously fixes the order one has to calculate in the KSW EFT so that \mathcal{R} is obtained up to the required precision. Following the same notation as for the KSW amplitudes, let us write:

$$\mathcal{R} = R_0 + R_1 + R_2 + R_3 + \mathcal{O}(p^4), \quad (2.14)$$

and $g(s) = M\nu/4\pi + iMp/4\pi - p^2/2\pi^2 + \mathcal{O}(p^4)$. Then we we must match:

$$\frac{1}{A_{S_0^1}^{KSW}} = \left(\frac{1}{A_{-1}}\right) - \left(\frac{A_0}{A_{-1}^2}\right) + \left(\frac{A_0^2 - A_1A_{-1}}{A_{-1}^3}\right) + \mathcal{O}(p^4), \quad (2.15)$$

with

$$\begin{aligned} -\left(\frac{1}{\mathcal{R}} + g\right) &= -\left(\frac{1}{R_0} + \frac{M\nu}{4\pi}\right) + \left(\frac{R_1}{R_0^2} - i\frac{Mp}{4\pi}\right) + \left(\frac{p^2}{2\pi^2} + \frac{R_0R_2 - R_1^2}{R_0^3}\right) + \left(\frac{R_1^3 - 2R_0R_1R_2 + R_0^2R_3}{R_0^4}\right) \\ &\quad + \mathcal{O}(p^4), \end{aligned} \quad (2.16)$$

where we have shown between brackets the different orders, from order p^0 up to order p^3 . As a result of the matching we can fix R_0 , R_1 , R_2 and R_3 in terms of ν , $A_{-1}(p)$, $A_0(p)$ and $A_1(p)$. We follow ref.[14] for expressing the KSW amplitudes, so that any of the previous amplitudes are scale independent at each order in the expansion.

Taking into account that

$$A_{-1} = -\frac{4\pi}{M} \frac{1}{\gamma + ip} , \quad (2.17)$$

with γ a quantity of order p , we can write the following expressions for the R_i :

$$\begin{aligned} R_0 &= -\frac{4\pi}{M\nu} , \\ R_1 &= -\frac{4\gamma\pi}{M\nu^2} , \\ R_2 &= -\frac{4(2\nu p^2 + \gamma^2 M\pi) + \nu(\frac{4\pi}{A_{-1}})^2 A_0(p)}{M^2\nu^3} , \\ R_3 &= -\frac{1}{4M^2\nu^4\pi} (8\gamma\nu(\frac{4\pi}{A_{-1}})^2\pi A_0(p) - \nu^2(\frac{4\pi}{A_{-1}})^3 A_0(p)^2 + 4\pi[4\gamma(4\nu p^2 + \gamma^2 M\pi) \\ &\quad + \nu^2(\frac{4\pi}{A_{-1}})^2 A_1(p)]) . \end{aligned} \quad (2.18)$$

Hence working at NLO, $\mathcal{O}(p^0)$, in the KSW amplitudes [13] we will have \mathcal{R} up to $\mathcal{O}(p^2)$, as explained above,

$$\mathcal{R}^{NLO} = R_0 + R_1 + R_2 , \quad (2.19)$$

and matching with the ones at NNLO [14], $\mathcal{O}(p)$, we calculate \mathcal{R} up to $\mathcal{O}(p^3)$:

$$\mathcal{R}^{NNLO} = R_0 + R_1 + R_2 + R_3 . \quad (2.20)$$

The resulting \mathcal{R} is substituted in eq.(2.5) and in this way we calculate the partial waves at the different orders considered so forth. It is clear that the process above can be done so as to match with a KSW amplitude calculated at any order. In this way the precision of the resulting amplitude is increased order by order.

Let us consider now in more detail the meaning of the kernel \mathcal{R} . Take first the simpler case of the pionless effective field theory, where only local interactions and even numbers of derivatives appear in the Lagrangians. For this case, the resulting partial waves have only the right hand cut and are free of crossed cuts due to the exchanges of other particles, being the pions the lightest ones. This is important for the nucleon-nucleon dynamics since at very low energies the pions can be treated as heavy particles and integrated out [26]. Thus, only local operators and the unitarity cut remain. We follow the line of reasoning of ref.[27], where the so important Castillejo-Dalitz-Dyson (CDD) poles were introduced. This reference was also used in ref.[18] in the context of chiral Lagrangians to show the general structure of a meson-meson partial wave with only the unitarity cut. Here we show the main points of the reasoning, for further details the reader is referred to ref.[18]. The idea is that when the partial wave $T_{L_j^{2S+1}, L_j^{2S+1}}$ has a zero then its inverse has a pole. This pole in the inverse of the partial wave can be on the real axis or in other place of the complex plane of the physical sheet ($\text{Imp} \geq 0$). Special care is needed when these poles lie

on the real axis above threshold since then eq.(2.1) can only be applied between any pair of such poles. These technical details are given in refs.[27, 18]. In this way, the inverse of the partial wave is a meromorphic function in the cut s plane from threshold to infinity. The net answer from a dispersion relation of the inverse of the amplitude, by applying the Cauchy theorem of integration to the circuit made up by the circle at infinity deformed to engulf the unitarity cut, is:

$$T_{L_J^{2S+1}, L_J^{2S+1}} = - \left(\sum_n \frac{\gamma_n}{s - s_n} + g \right)^{-1}, \quad (2.21)$$

where the poles present in the sum are the so called CDD poles [27]. The sum is what we have denoted before in eq.(2.5) by $1/\mathcal{R}$. Let us note that in the pionless effective field theory supplied with the PDS scheme, the Schrödinger equation can be solved straightforwardly and results [13]:

$$A = - \left(\frac{1}{\sum_{m=0} C_{2m} p^{2m}} + \frac{M}{4\pi} (\mu + ip) \right)^{-1}, \quad (2.22)$$

with A being the same partial wave as $T_{L_J^{2S+1}, L_J^{2S+1}}$. Comparing this equation with eq.(2.21), one has:

$$\frac{1}{\mathcal{R}} = \sum_n \frac{\gamma_n}{s - s_n} = \frac{1}{\sum_{m=0} C'_{2m} p^{2m}} + \frac{M}{4\pi} (\mu - \nu) = \frac{1}{\sum_{m=0} C'_m p^{2m}}, \quad (2.23)$$

where we have omitted in the previous equation the relativistic corrections in g from the logarithmic term in eq.(2.4). The C'_m are given in terms of the C_m so as to reabsorb the constant term in the sum. One can always choose the s_n and γ_n so that the previous equality holds.^{#4}. This is why we have written finally $1/\mathcal{R}$ in eq.(2.5), instead of simply \mathcal{R} , because at the tree level, omitting the g function in eq.(2.21), one has $T_{L_J^{2S+1}, L_J^{2S+1}} = \mathcal{R}$. Let us note in addition that $-\mathcal{R}$ can be identified with the renormalized potential if we rewrite $T = -1/(1/\mathcal{R} + g)$ as:

$$T = -\mathcal{R} - \mathcal{R} g T, \quad (2.24)$$

like an ordinary Lippmann-Schwinger equation with an on-shell potential $V \equiv -\mathcal{R}$. Let us remind, as stated above, that g is just the unitarity bubble iterated when solving a Lippmann-Schwinger equation.

When the pions are included in the formalism, the interacting kernel \mathcal{R} contains apart from a *finite* sum of local terms, like those of eq.(2.23), other contributions coming from the exchange of pions which give rise to crossed cuts. All these contributions are included *perturbatively* when \mathcal{R} is fixed by matching the expansion of the inverse of eq.(2.5) with the expansions of the inverses of the KSW partial waves. Let us stress that the entire formalism is algebraic since the interacting kernel \mathcal{R} is on-shell. This notorious simplicity of our approach compared to that of refs.[5, 6, 12] is a result of resumming the unitarity bubbles by making use of analyticity and unitarity that only involve on-shell amplitudes. One needs to realize that for resumming the large factors $2M/p$ associated with two-nucleon intermediate states, whose necessity was stressed in ref.[5], there are

^{#4}For example, prove the above equality by considering first that the sum on the right hand side just contains two terms. Then, for the general case, it is easily seen, by recurrence to the case with one term less in the sum, that the equality holds. Note that when $s_n \rightarrow \infty$ the corresponding CDD pole just gives rise to a constant

several possibilities. One way is to solve the Lippmann-Schwinger equation [5, 6, 12], but there is another standard method based on the separation of cuts resulting from S-matrix theory, this is the N/D method [17] that we follow here.

2.2 $S_1^3-D_1^3$ coupled partial waves

The resulting expressions to match between are the expansions of the matrix elements of the inverse of the KSW matrix of partial waves for the $S_1^3 - D_1^3$ sector, $A_{S_1^3-D_1^3}^{KSW}$:

$$\begin{aligned}
(A_{S_1^3-D_1^3}^{KSW})_{11}^{-1} &= \left(\frac{1}{A_{11,-1}} \right) + \left(\frac{A_{12,0}^2 - A_{11,0}A_{22,0}}{A_{11,-1}^2 A_{22,0}} \right) \\
&+ \left(\frac{A_{12,0}^4 + 2A_{11,-1}A_{12,0}A_{12,1}A_{22,0} + (A_{11,0}^2 - A_{11,-1}A_{11,1})A_{22,0}^2}{A_{11,-1}^3 A_{22,0}^2} \right. \\
&- \left. \frac{A_{12,0}^2(2A_{11,0}A_{22,0} + A_{11,-1}A_{22,1})}{A_{11,-1}^3 A_{22,0}^2} \right) + \mathcal{O}(p^4), \\
(A_{S_1^3-D_1^3}^{KSW})_{12}^{-1} &= - \left(\frac{A_{12,0}}{A_{11,-1}A_{22,0}} \right) - \left(\frac{A_{12,0}^3 + A_{11,-1}A_{12,1}A_{22,0} - A_{12,0}(A_{11,0}A_{22,0} + A_{11,-1}A_{22,1})}{A_{11,-1}^2 A_{22,0}^2} \right) \\
&+ \mathcal{O}(p^3), \\
(A_{S_1^3-D_1^3}^{KSW})_{22}^{-1} &= \left(\frac{1}{A_{22,0}} \right) + \left(\frac{A_{12,0}^2 - A_{11,-1}A_{22,1}}{A_{11,-1}A_{22,0}^2} \right) + \mathcal{O}(p^2), \tag{2.25}
\end{aligned}$$

and the ones that result from the expansion of eq.(2.5). In this case \mathcal{R} is a 2×2 symmetric matrix:

$$\mathcal{R} = \begin{pmatrix} R_{11} & R_{12} \\ R_{12} & R_{22} \end{pmatrix}, \tag{2.26}$$

and $g(s) = \text{diagonal}(g_1(s), g_2(s))$ with its associated subtraction constants ν_1 and ν_2 . Like in the S_0^1 channel we will take $g_i = \mathcal{O}(p^0)$ and $R_{11} = R_{11,0} + R_{11,1} + R_{11,2} + R_{11,3} + \mathcal{O}(p^4)$. In the KSW scheme at the leading order the S_1^3 and D_1^3 are uncoupled and the mixing starts at NLO, one order higher. Thus, we take $R_{12} = R_{12,1} + R_{12,2} + \mathcal{O}(p^3)$, starting one order higher than R_{11} . Finally, since the D_1^3 partial wave starts at order p^0 , and is free of unnatural scattering lengths, we take then $R_{22} = R_{22,0} + R_{22,1} + \mathcal{O}(p^2)$. The expansion of the inverse of eq.(2.5) is now straightforward and one obtains:

$$\begin{aligned}
(T^{31})_{11}^{-1} &= - \left(\frac{M\nu_1}{4\pi} + \frac{1}{R_{11,0}} \right) + \left(\frac{R_{11,1}}{R_{11,0}^2} - i \frac{Mp}{4\pi} \right) + \left(\frac{p^2}{2\pi^2} + \frac{R_{11,0}R_{11,2}R_{22,0} - R_{11,1}^2 R_{22,0} - R_{11,0}R_{12,1}^2}{R_{11,0}^3 R_{22,0}} \right) \\
&- \left(\frac{-R_{11,1}^3 R_{22,0}^2 + 2R_{11,0}R_{11,1}R_{22,0}(-R_{12,1}^2 + R_{11,2}R_{22,0})}{R_{11,0}^4 R_{22,0}^2} \right. \\
&- \left. \frac{R_{11,0}^2(-2R_{12,1}R_{12,2}R_{22,0} + R_{11,3}R_{22,0}^2 + R_{12,1}^2 R_{22,1})}{R_{11,0}^4 R_{22,0}^2} \right) + \mathcal{O}(p^4), \\
(T^{31})_{12}^{-1} &= \left(\frac{R_{12,1}}{R_{11,0}R_{22,0}} \right) - \left(\frac{R_{11,1}R_{12,1}R_{22,0} - R_{11,0}R_{12,2}R_{22,0} + R_{11,0}R_{12,1}R_{22,1}}{R_{11,0}^2 R_{22,0}^2} \right) + \mathcal{O}(p^3),
\end{aligned}$$

$$(T^{31})_{22}^{-1} = -\left(\frac{M\nu_2}{4\pi} + \frac{1}{R_{22,0}}\right) + \left(\frac{R_{22,1}}{R_{22,0}^2} - i\frac{Mp}{4\pi}\right) + \mathcal{O}(p^2). \quad (2.27)$$

We can then easily solve for the $R_{ij,k}$ and we obtain:

$$\begin{aligned} R_{11,0} &= -\frac{4\pi}{M\nu_1}, \\ R_{11,1} &= -\frac{4\gamma\pi}{M\nu_1^2}, \\ R_{11,2} &= \frac{1}{M^2\nu_1^3(4\pi + M\nu_2A_{22,0})} \left\{ M^3\nu_1\nu_2(\gamma + ip)^2 A_{12,0}^2 - 4(2\nu_1p^2 + \gamma^2 M\pi)(4\pi + M\nu_2A_{22,0}) \right. \\ &\quad \left. - M^2\nu_1(\gamma + ip)^2 A_{11,0}(4\pi + M\nu_2A_{22,0}) \right\}, \\ R_{11,3} &= \frac{1}{4M\nu_1^3\pi A_{22,0}^2} \left\{ -M(\gamma + ip)^2(M(\gamma + ip)A_{12,0}^4 - 8\pi A_{12,0}A_{12,1}A_{22,0} + (M(\gamma + ip)A_{11,0}^2 \right. \\ &\quad + 4\pi A_{11,1})A_{22,0}^2 - 2A_{12,0}^2(M(\gamma + ip)A_{11,0}A_{22,0} - 2\pi A_{22,1})) + \frac{1}{\nu_1^2(4\pi + M\nu_2A_{22,0})^2} \left(\right. \\ &\quad \times 8\pi(2\gamma^3\pi A_{22,0}^2(4\pi + M\nu_2A_{22,0})^2 - \frac{1}{M}(\gamma A_{22,0}(4\pi + M\nu_2A_{22,0})^2(-M^2\nu_1(\gamma + ip)^2 A_{12,0}^2 \\ &\quad + (4(2\nu_1p^2 + \gamma^2 M\pi) + M^2\nu_1(\gamma + ip)^2 A_{11,0})A_{22,0})) - M\nu_1(\gamma + ip)^2 A_{12,0}(-M\nu_1(\gamma + ip)A_{12,0}^3 \\ &\quad \times (2\pi + M\nu_2A_{22,0}) + 4\nu_1\pi A_{12,1}A_{22,0}(4\pi + M\nu_2A_{22,0}) + A_{12,0}(M(4\gamma\nu_2\pi - 2i\nu_1p\pi \\ &\quad + M\nu_1\nu_2(\gamma + ip)A_{11,0})A_{22,0}^2 - 8\nu_1\pi^2 A_{22,1} + 4\pi A_{22,0}(4\gamma\pi + M\nu_1(\gamma + ip)A_{11,0} \\ &\quad \left. \left. - M\nu_1\nu_2A_{22,1})))) \right) \right\}, \\ R_{12,1} &= \frac{4(\gamma + ip)\pi A_{12,0}}{\nu_1(4\pi + M\nu_2A_{22,0})}, \\ R_{12,2} &= \frac{1}{\nu_1^2(4\pi + M\nu_2A_{22,0})^2} \left\{ (\gamma + ip)(-M^2\nu_1\nu_2(\gamma + ip)A_{12,0}^3 + 4\nu_1\pi A_{12,1}(4\pi + M\nu_2A_{22,0}) \right. \\ &\quad \left. + A_{12,0}(M\nu_1(\gamma + ip)A_{11,0}(4\pi + M\nu_2A_{22,0}) + 4\pi(4\gamma\pi + M(\gamma\nu_2 - i\nu_1p)A_{22,0} - M\nu_1\nu_2A_{22,1})) \right\}, \\ R_{22,0} &= -\frac{4\pi A_{22,0}}{4\pi + M\nu_2A_{22,0}}, \\ R_{22,1} &= -\frac{4\pi(M(\gamma + ip)A_{12,0}^2 - iMpA_{22,0}^2 + 4\pi A_{22,1})}{(4\pi + M\nu_2A_{22,0})^2}. \end{aligned} \quad (2.28)$$

Similarly as in the S_0^1 case, working at NLO implies:

$$\begin{aligned} R_{11}^{NLO} &= R_{11,0} + R_{11,1} + R_{11,2}, \\ R_{12}^{NLO} &= R_{12,1}, \\ R_{22}^{NLO} &= R_{22,0}, \end{aligned} \quad (2.29)$$

and at NNLO:

$$\begin{aligned} R_{11}^{NNLO} &= R_{11,0} + R_{11,1} + R_{11,2} + R_{11,3}, \\ R_{12}^{NNLO} &= R_{12,1} + R_{12,2}, \\ R_{22}^{NNLO} &= R_{22,0} + R_{22,1}. \end{aligned} \quad (2.30)$$

2.3 P , D , F_2^3 and G_3^3 partial waves except D_1^3

For the P and D waves, the NLO KSW amplitudes [13] just contain one pion exchange (OPE) and at NNLO [14, 25] they only include in addition the reducible part of the twice iterated OPE. The physics behind this is then quite limited and will show up in the phenomenology which, on the other hand, is of the same quality as that of the LO Weinberg's scheme results, ref.[12]. Indeed, at LO the potential within the Weinberg's scheme just contains OPE (our order p^0 contribution) while the reducible part of the twice iterated OPE is generated by solving the Schrödinger equation. For these partial waves, which are free from enhancements due to unnatural scattering lengths, the formalism simplifies since the scaling of the counterterms is just given by dimensional analysis and there are no KSW amplitudes of order p^{-1} . For the elastic ones, $\mathcal{R} = R_0 + R_1 + \mathcal{O}(p^2)$ and $g = \mathcal{O}(p^0)$ and for the coupled channel partial waves, namely $F_2^3 - F_2^3$ and $D_3^3 - G_3^3$, $R_{ij} = R_{ij,0} + R_{ij,1} + \mathcal{O}(p^2)$ and $g_i(s) = \mathcal{O}(p^0)$, since all the channels start to contribute at the same order p^0 and as stated they are free of unnatural scattering lengths.

For the partial waves without coupled channels, after performing the appropriate KSW expansion and matching with the inverse of the KSW amplitude, as done previously, one can write:

$$\begin{aligned} R_0 &= -\frac{A_0}{1 + A_0 \frac{M\nu}{4\pi}} , \\ R_1 &= -\frac{1}{(1 + A_0 \frac{M\nu}{4\pi})^2} (A_1 - i \frac{pM}{4\pi} A_0^2) , \end{aligned} \quad (2.31)$$

so that,

$$\begin{aligned} \mathcal{R}^{NLO} &= R_0 , \\ \mathcal{R}^{NNLO} &= R_0 + R_1 . \end{aligned} \quad (2.32)$$

For the two coupled channel partial waves, the chiral expansion is performed in coupled channels. Taking into account that $R_{ij} = R_{ij,0} + R_{ij,1} + \mathcal{O}(p^2)$, as discussed, one has:

$$\begin{aligned} R_{11,0} &= -\frac{4\pi(4\pi A_{11,0} - M\nu_2 A_{12,0}^2 + M\nu_2 A_{11,0} A_{22,0})}{(4\pi + M\nu_1 A_{11,0})(4\pi + M\nu_2 A_{22,0}) - M^2 \nu_1 \nu_2 A_{12,0}^2} , \\ R_{11,1} &= \frac{1}{[M^2 \nu_1 \nu_2 A_{12,0}^2 - (4\pi + M\nu_1 A_{11,0})(4\pi + M\nu_2 A_{22,0})]^2} \left\{ 4i\pi(4i\pi A_{11,1}(4\pi + M\nu_2 A_{22,0})^2 \right. \\ &\quad + M(M^2 \nu_2^2 p A_{12,0}^4 - 8i\nu_2 \pi A_{12,1} A_{12,0}(4\pi + M\nu_2 A_{22,0}) + p A_{11,0}^2 (4\pi + M\nu_2 A_{22,0})^2 \\ &\quad \left. - 2A_{12,0}^2 (-2iM\nu_2^2 \pi A_{22,1} + p(4\pi(-2\pi + M\nu_2 A_{11,0}) + M^2 \nu_2^2 A_{11,0} A_{22,0}))) \right\} , \\ R_{12,0} &= -\frac{16\pi^2 A_{12,0}}{(4\pi + M\nu_1 A_{11,0})(4\pi + M\nu_2 A_{22,0}) - M^2 \nu_1 \nu_2 A_{12,0}^2} , \\ R_{12,1} &= -\frac{1}{[M^2 \nu_1 \nu_2 A_{12,0}^2 - (4\pi + M\nu_1 A_{11,0})(4\pi + M\nu_2 A_{22,0})]^2} \left\{ 16\pi^2 (A_{12,1} (M^2 \nu_1 \nu_2 A_{12,0}^2 \right. \\ &\quad + (4\pi + M\nu_1 A_{11,0})(4\pi + M\nu_2 A_{22,0})) + iM A_{12,0} (-4p\pi A_{11,0} + M(\nu_1 + \nu_2) p A_{12,0}^2 + 4i\nu_2 \pi A_{22,1} \\ &\quad \left. + iM\nu_1 \nu_2 A_{11,0} A_{22,1} - 4p\pi A_{22,0} - M\nu_1 p A_{11,0} A_{22,0} - M\nu_2 p A_{11,0} A_{22,0} \right\} , \end{aligned}$$

$$\begin{aligned}
& + i\nu_1 A_{22,1}(4\pi + M\nu_2 A_{22,0}))\} , \\
R_{22,0} &= -\frac{4\pi(-M\nu_1 A_{12,0}^2 + (4\pi + M\nu_1 A_{11,0})A_{22,0})}{(4\pi + M\nu_1 A_{11,0})(4\pi + M\nu_2 A_{22,0}) - M^2\nu_1\nu_2 A_{12,0}^2} , \\
R_{22,1} &= \frac{1}{[M^2\nu_1\nu_2 A_{12,0}^2 - (4\pi + M\nu_1 A_{11,0})(4\pi + M\nu_2 A_{22,0})]^2} \{4i\pi(-8iM\nu_1\pi(4\pi + M\nu_1 A_{11,0})A_{12,1}A_{12,0} \\
& + M^3\nu_1^2 p A_{12,0}^4 + (4\pi + M\nu_1 A_{11,0})^2(4i\pi A_{22,1} + MpA_{22,0}^2) - 2MA_{12,0}^2(-2iM\nu_1^2\pi A_{11,1} \\
& + p(-8\pi^2 + M\nu_1(4\pi + M\nu_1 A_{11,0})A_{22,0}))\} , \tag{2.33}
\end{aligned}$$

where the subscript 1 before the period always refers to the channel with lower orbital angular momentum and 2 to the highest one.

Working at NLO implies taking:

$$\begin{aligned}
R_{11}^{NLO} &= R_{11,0} , \\
R_{12}^{NLO} &= R_{12,0} , \\
R_{22}^{NLO} &= R_{22,0} , \tag{2.34}
\end{aligned}$$

and at NNLO:

$$\begin{aligned}
R_{11}^{NNLO} &= R_{11,0} + R_{11,1} , \\
R_{12}^{NNLO} &= R_{12,0} + R_{12,1} , \\
R_{22}^{NNLO} &= R_{22,0} + R_{22,1} . \tag{2.35}
\end{aligned}$$

As a check for all the previous expressions for the interacting kernel \mathcal{R} , we have explicitly verified that they are real in the physical nucleon-nucleon region, p real and positive, and furthermore they also have the correct KSW order, as they should.

3 Results and discussion

In this section we consider the phenomenological applications of the previous scheme to the S and higher partial waves. Of particular relevance is to study the triplet S-wave channel, S_1^3 , and its mixing with the D_1^3 , since here the KSW amplitudes do not converge for $p \gtrsim 100$ MeV although pions are explicitly included. We first discuss the S_0^1 channel and then consider the S_1^3 coupled with the D_1^3 partial wave. After that we turn to discuss the P , D , F_2^3 and G_3^3 waves and compare with other approaches.

3.1 S_0^1 channel

We follow the notation of ref.[14] for the KSW amplitudes, where only those combinations of counterterms that appear in a given amplitude are shown and are denoted by ξ_i . At NLO we have two of such counterterms, ξ_1 and ξ_2 together with γ that already appears at LO. We express these two counterterms in terms of γ by performing the ERE in eq.(2.5), with \mathcal{R}^{NLO} given in eq.(2.19),

reproducing the physical values of the scattering length, a_s , and effective range, r_0 . We then have:

$$\begin{aligned}\xi_1 &= \frac{-g_A^2 M^2 (6\gamma^2 - 8\gamma m_\pi + 3m_\pi^2)(-1 + a_s \nu)^2 + 12f^2 m_\pi^2 (4 - 8a_s \nu + a_s^2 M \nu^2 \pi r_0)}{96f^2 m_\pi^2 (-1 + a_s \nu)^2 \pi^2}, \\ \xi_2 &= \frac{M(g_A^2 \gamma M(\gamma - 2m_\pi)\nu(-1 + a_s \nu) + 8f^2(-\nu^2 + \gamma^2(-1 + a_s \nu) + \gamma\nu(-1 + a_s \nu))\pi)}{32f^2 m_\pi^2 \nu(-1 + a_s \nu)\pi^2}.\end{aligned}\quad (3.1)$$

At NNLO there are three more counterterms, ξ_3 , ξ_4 and ξ_5 . Once the renormalization group equations are solved within the KSW perturbative scheme, ξ_5 results to be a higher order counterterm and must be set equal to zero at NNLO. We will show below, when discussing the results for the $S_1^3 - D_1^3$ channel after eq.(3.15), that indeed, ξ_5 must be left as a free parameter within our scheme. Nevertheless, we found after performing fits with ξ_5 free, that it turns out to be negligibly small in any case, so that in the following we also make $\xi_5 = 0$ for this channel as in the pure KSW treatment [14]. We then fix the counterterms ξ_3 and ξ_4 in terms of ξ_1 , ξ_2 , γ , a_s and r_0 by performing the ERE. The expressions of ξ_3 and ξ_4 in terms of ξ_1 , ξ_2 , γ , a_s and r_0 are:

$$\begin{aligned}\xi_3 &= \frac{1}{1536f^4 m_\pi^2 \nu^2 (-1 + a_s \nu)\pi^3} \{48f^2 g_A^2 M \nu (-1 + a_s \nu)\pi(2\gamma^3 M + \gamma^2 M(-4m_\pi + \nu) + 8m_\pi^3 \nu \pi \xi_2 \\ &- 2\gamma m_\pi \nu(M + 4m_\pi \pi \xi_2)) - 384f^4 \pi^2(\gamma^2 M \nu(1 - a_s \nu) + \gamma^3(M - a_s M \nu) - \gamma\nu(-1 + a_s \nu) \\ &\times (M\nu - 8m_\pi^2 \pi \xi_2) + \nu^2(M\nu + 4m_\pi^2(-1 + a_s \nu)\pi \xi_2)) + g_A^4 M^3 \nu^2(-1 + a_s \nu)(6\gamma^3 - 21\gamma^2 m_\pi \\ &- \gamma m_\pi^2(-18 + \log(4096)) + m_\pi^3 \log(4096))\}, \\ \xi_4 &= -\frac{1}{3072f^4 m_\pi^2 \nu(-1 + a_s \nu)^2 \pi^3} \{384f^4 m_\pi^2 \pi(8\gamma(-1 + a_s \nu)^2(-1 + 2\pi^2 \xi_1) + \nu(-4 + 8\pi^2 \xi_1 \\ &+ a_s^2 \nu^2 \pi(-M r_0 + 8\pi \xi_1) + 8a_s \nu(1 - 2\pi^2 \xi_1))) + 32f^2 g_A^2 M(-1 + a_s \nu)^2 \pi(12\gamma^3 M + \gamma^2 M(-16m_\pi + 6\nu) \\ &+ 2\gamma m_\pi(M(3m_\pi - 4\nu) + 12m_\pi \nu \pi(\xi_1 - 2\xi_2)) + m_\pi^2 \nu(3M + 8m_\pi \pi(-3\xi_1 + 4\xi_2))) \\ &+ g_A^4 M^3 \nu(-1 + a_s \nu)^2(48\gamma^3 - 135\gamma^2 m_\pi + 2m_\pi^3(-13 + 4\log(16)) - 4\gamma m_\pi^2(-27 + \log(4096)))\}.\end{aligned}\quad (3.2)$$

The values for the parameters that we take are $f = 130.67$ MeV, $g_A = 1.267$, $m_\pi = 138$ MeV, $M = 939$ MeV. Specifically for the S_0^1 channel, the ERE parameters are $a_s = -23.714$ fm and $r_0 = 2.73$ fm. On the other hand, since a_s is so large in this channel, and γ is around $1/a_s$ both in KSW as in our approach,^{#5} in the following we take directly $\gamma = 0$.

In the KSW approach at NLO one has the free parameters γ , ξ_1 and ξ_2 . In ref.[14] γ is fixed by requiring the presence of a pole in the unphysical sheet in the position required by the ERE, just below threshold. Then ξ_2 is fixed in terms of ξ_1 to avoid spurious poles that appear at NLO (double poles). As a result only ξ_1 is taken as free in the fit to the elastic S_0^1 phase shifts in ref.[14]. The resulting values are:

$$\gamma^* = -7.88 \text{ fm}^{-1}, \quad \xi_1 = 0.22, \quad \xi_2^* = 0.03, \quad (3.3)$$

where those parameters marked with a star are not taken as free ones in the fit. The corresponding curve is the dotted one in the left panel of fig.1. In the approach that we present here we have

^{#5}For example, just take $\mathcal{R}^{LO} = R_0 + R_1$ in eq.(2.5) and then perform the ERE, with R_0 and R_1 given in eq.(2.18).

one more parameter at NLO, ν . Since, as discussed above, we have fixed $\gamma = 0$ and ξ_1 and ξ_2 are calculated from the ERE, eq.(3.1), only ν would be free in the fit. Instead of performing a fit, and in order to show as well the sensitivity of our results at NLO under changes of the subtraction constant ν , we show in the left panel of fig.1 two curves corresponding to $\nu = 200$ (solid line) and $\nu = 900$ MeV (dashed line). The solid curve reproduces already very well the data for $p \lesssim 150$ MeV. The calculated counterterms are $\xi_1^* = 0.22(0.25)$, $\xi_2^* = 0.03(0.03)$ for $\nu = 200(900)$. Taking into account table 1 we see that the considered variation of ν implies a large change of the hypothetical cut-off from around 300 MeV to values around 2 GeV. It is also worth mentioning the constancy of the values of the counterterms ξ_1 and ξ_2 . This is just a consequence of the fact that $\nu a_s \gg 1$ as can be seen from eq.(3.1).

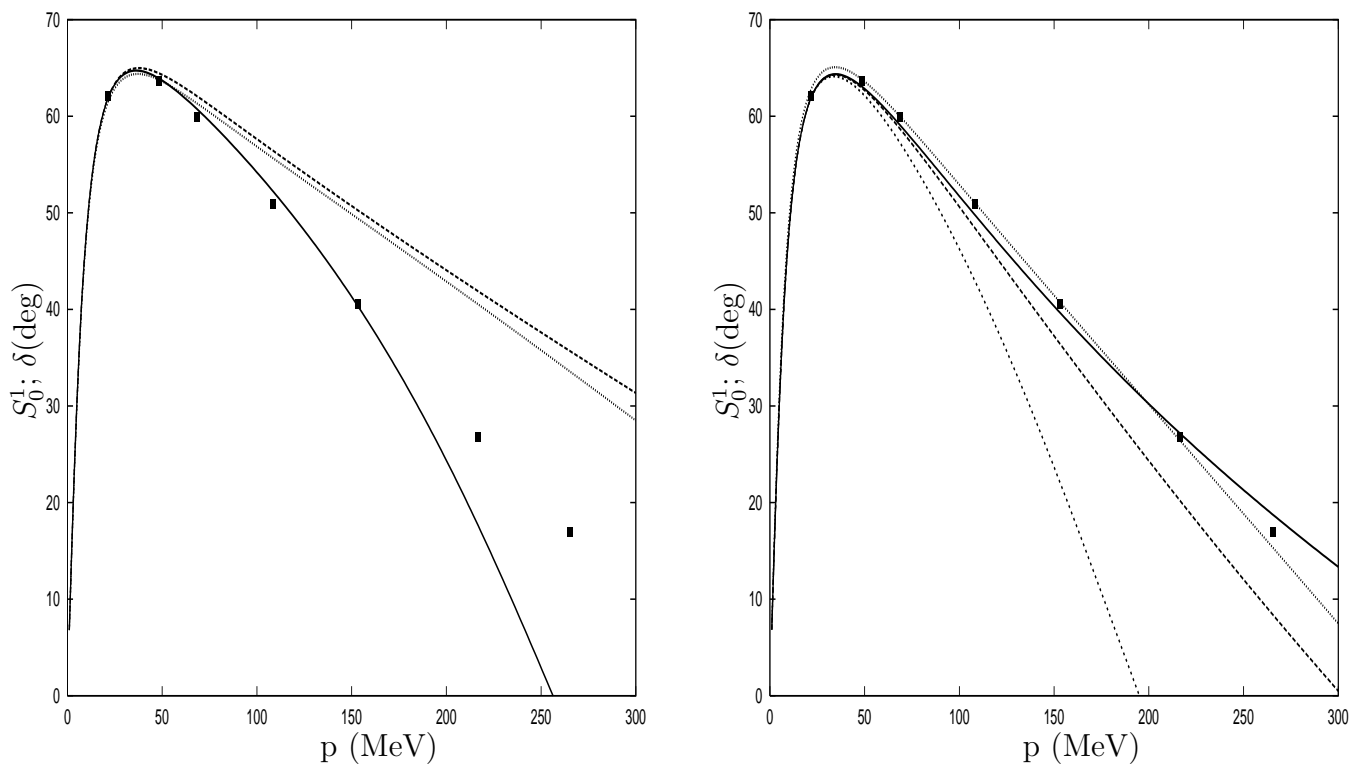


Figure 1: Phase shifts for the S_0^1 channel. The dotted lines in the left and right panels are the NLO/NNLO KSW results [14], respectively. Left panel: The solid and dashed lines represent the NLO results of our approach with $\nu = 200$ MeV and 900 MeV, respectively. Right panel: The solid line is the fit of eq.(3.5). The dashed and short-dashed lines are our NNLO results with $\nu = 500$ MeV and 200 MeV, in order. The data are from the Nijmegen partial wave analysis, ref.[24].

Let us consider now the NNLO results both from the pure KSW approach and ours. At this order three new counterterms appear, ξ_3 , ξ_4 and ξ_5 . Because ξ_5 is a higher order counterterm is fixed at zero in ref.[14]. On the other hand, by imposing, as in the NLO case, the absence of double and triple poles one can express ξ_3 in terms of ξ_4 . As a result only two free parameters are left to fit the data. The resulting values from ref.[14] are:

$$\gamma^* = -7.88 \text{ fm}^{-1}, \quad \xi_1 = 0.078, \quad \xi_2^* = 0.03, \quad \xi_3^* = 0.18, \quad \xi_4 = 0.25. \quad (3.4)$$

The generated curve is the dotted one in the right panel of fig.1 which indeed reproduces the data rather accurately. We now come to our approach. As stated, ξ_3 and ξ_4 are fixed in terms of γ , ξ_1 , ξ_2 , a_s and r_0 by eqs.(3.2). As in the NLO case ξ_1 and ξ_2 are fixed by eq.(3.1) and $\gamma = 0$. As a result we have only one free parameter, ν . After performing the fit to the phase shifts one has the values:

$$\gamma^* = 0 \text{ fm}^{-1}, \quad \xi_1^* = 0.25, \quad \xi_2^* = 0.03, \quad \xi_3^* = 0.21, \quad \xi_4^* = 0.24 \quad \nu = 870 \text{ MeV}, \quad (3.5)$$

corresponding to the solid line in the right panel of fig.1, which is quite similar to the NNLO KSW one with two free parameters although not so close to all the data points. In addition we show by the dashed and short-dashed lines those curves that result from our formalism keeping ν fixed at the values 500 MeV and 200 MeV, respectively. The variation in the results from changes of ν is similar to that obtained at the NLO, although the quality of the reproduction of data have improved.

We now consider as well the possibility of fixing ν and then fitting ξ_1 and ξ_2 while ξ_3 and ξ_4 are calculated once more from eqs.(3.2). We take the set of values $\nu = 200, 500, 700$ and 900 MeV that are shown in the left panel of fig.2 by the short dashed, dot-dashed, solid and dashed lines, respectively, although cannot be distinguished. In addition we also show the dotted line corresponding to the NNLO results within the KSW approach from ref.[14]. We see that basically there is no dependence on ν although the values of the fitted counterterms change substantially and they are in order, for $\nu = 200, 500, 700, 900$ MeV: $\xi_1 = -0.53, 0.14, 0.56, 0.87$ and $\xi_2 = -0.21, 0.04, 0.23, 0.36$. On the other hand, the reproduction of data is very good.

Let us now go to higher energies and show results up to laboratory kinetic energies, $T_{lab}=350$ MeV (the threshold for pion production is at $T_{lab} = 280$ MeV). This is given in the right panel of fig.2. The solid line corresponds to the solid one of the left panel of the same figure, that is, when fixing $\nu = 700$ MeV and ξ_1 and ξ_2 taken as free parameters (as shown in the left panel of fig.2 the change from one value of ν to another is almost negligible). In addition, the dashed line is the solid one of the right panel of fig.1, eq.(3.5). The short dashed line is calculated at NLO within our approach with $\nu = 200$ MeV (solid line in the left panel of fig.1) and the NLO KSW results of ref.[14] are given by the dotted line.

3.2 $S_1^3 - D_1^3$ coupled channels

We treat the counterterms in analogous lines as described above for the S_0^1 channel, although now γ and ξ_5 are taken as free parameters. In addition, at NNLO in KSW there is a new parameter in this channel, ξ_6 , related to the $S_1^3 - D_1^3$ mixing. One should take into account that although we use the same names for γ and the ξ 's counterterms as in the S_0^1 case, they are indeed different [13, 14]. As before ξ_1 and ξ_2 are given at NLO in terms of γ , a_s and r_0 from the ERE. At NNLO we then calculate ξ_3 and ξ_4 from ξ_1 , ξ_2 , γ , a_s and r_0 , independently of whether ξ_1 and ξ_2 are either taken as free parameters or fixed at NLO from ERE. The expressions for ξ_1 , ξ_2 , ξ_3 and ξ_4 determined from the ERE are the following:

$$\xi_1 = \frac{1}{96f^2m_\pi^2(-1+a_s\nu_1)^2\pi^2} \left\{ -g_A^2 M^2(6\gamma^2 - 8\gamma m_\pi + 3m_\pi^2)(-1+a_s\nu_1)^2 + 12f^2m_\pi^2(4 - 8a_s\nu_1 + a_s^2M\nu_1^2\pi r_0) \right\},$$

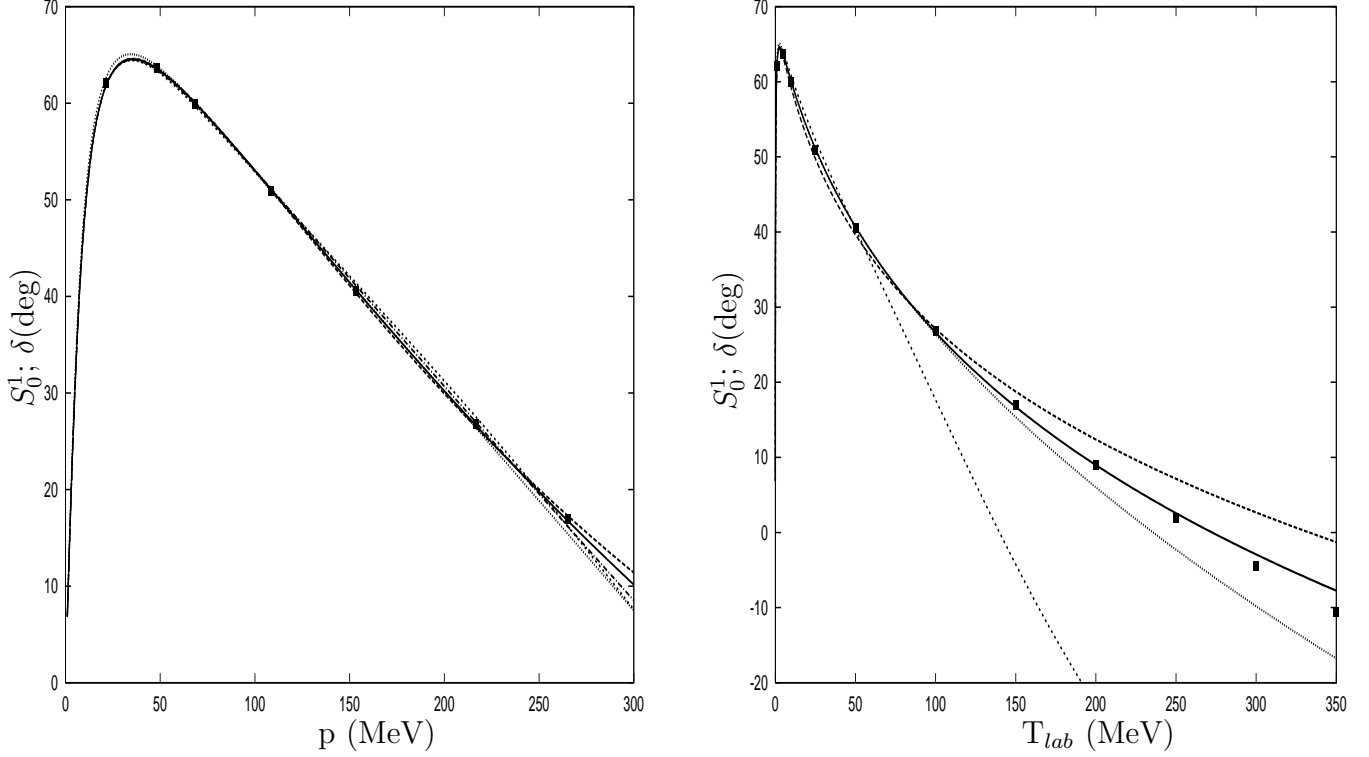


Figure 2: Phase shifts for the S_0^1 channel. The dotted lines are the NNLO results from the pure KSW approach [14]. The rest of the curves are calculated within our scheme. Left panel: The different curves are hardly distinguishable. The short-dashed, dot-dashed, solid and dashed curves are our NNLO with ν taken as 200, 500, 700, and 900 MeV, respectively. ξ_1 and ξ_2 are taken as free parameters. The right panel corresponds to higher energies with the phase shifts as function of T_{lab} . The solid line is the solid one of the left panel. The dashed line is the fit given in eq.(3.5) at NNLO and the short-dashed one is the solid line of the left panel of fig.1 calculated at NLO with ν fixed at 200 MeV. The data correspond to the Nijmegen partial wave analysis, ref.[24].

$$\xi_2 = \frac{1}{32f^2m_\pi^2\nu_1(-1+a_s\nu_1)\pi^2} \left\{ M(g_A^2\gamma M(\gamma-2m_\pi)\nu_1(-1+a_s\nu_1) + 8f^2(-\nu_1^2 + \gamma^2(-1+a_s\nu_1) + \gamma\nu_1(-1+a_s\nu_1))\pi) \right\}, \quad (3.6)$$

$$\xi_3 = \frac{1}{2560f^4m_\pi^2\nu_1^2(-1+a_s\nu_1)\pi^3} \left\{ 80f^2g_A^2M\nu_1(-1+a_s\nu_1)\pi(2\gamma^3M + \gamma^2M(-4m_\pi + \nu_1) + 8m_\pi^3\nu_1\pi\xi_2 - 2\gamma m_\pi\nu_1(M + 4m_\pi\pi\xi_2)) - 640f^4\pi^2(\gamma^2M\nu_1(1-a_s\nu_1) + \gamma^3(M - a_sM\nu_1) - \gamma\nu_1(-1+a_s\nu_1)) \times (M\nu_1 - 8m_\pi^2\pi\xi_2) + \nu_1^2(M\nu_1 + 4m_\pi^2(-1+a_s\nu_1)\pi\xi_2) + g_A^4M^3\nu_1^2(-1+a_s\nu_1)(10\gamma^3 - 95\gamma^2m_\pi - 5\gamma m_\pi^2(-15 + \log(4096)) + 2m_\pi^3(-8 + \log(67108864))) \right\},$$

$$\xi_4 = -\frac{1}{107520f^4m_\pi^2\nu_1(-1+a_s\nu_1)^2\pi^3} \left\{ 13440f^4m_\pi^2\pi(8\gamma(-1+a_s\nu_1)^2(-1+2\pi^2\xi_1) + \nu_1(-4+8\pi^2\xi_1 + a_s^2\nu_1^2\pi(-Mr_0 + 8\pi\xi_1) + 8a_s\nu_1(1-2\pi^2\xi_1))) + 1120f^2g_A^2M(-1+a_s\nu_1)^2\pi(12\gamma^3M + \gamma^2M(-16m_\pi$$

$$\begin{aligned}
& + 6\nu_1) + 2\gamma m_\pi (M(3m_\pi - 4\nu_1) + 12m_\pi \nu_1 \pi (\xi_1 - 2\xi_2)) + m_\pi^2 \nu_1 (3M + 8m_\pi \pi (-3\xi_1 + 4\xi_2))) \\
& + g_A^4 M^3 \nu_1 (-1 + a_s \nu_1)^2 (1680\gamma^3 - 3325\gamma^2 m_\pi - 6m_\pi^3 (913 + 1248 \log(2) + 280 \log(4) - 336 \log(16) \\
& - 140 \log(256)) - 840\gamma m_\pi^2 (-12 + \log(256))) \} . \tag{3.7}
\end{aligned}$$

At NLO the free parameters are γ , ξ_1 , ξ_2 , ν_1 and ν_2 while in the pure perturbative treatment of ref.[13, 14] the latter two are absent. In ref.[14] γ is fixed by requiring the presence of the deuteron pole in the physical sheet and ξ_2 is given in terms of ξ_1 in order to avoid double poles. As a result only one free parameter remains at this order in the KSW scheme, ξ_1 . This is fitted to the low energy S_1^3 elastic phase shifts for $p \leq 80$ MeV in ref.[14] with the resulting values [14]:

$$\gamma^* = 0.23 \text{ fm}^{-1}, \quad \xi_1 = 0.327, \quad \xi_2^* = -0.0936, \tag{3.8}$$

where as usual the stars indicate that γ and ξ_2 are not free parameters in the fit. The results are given by the dotted line in fig.3 both for the S_1^3 elastic phase shifts and for the ϵ_1 mixing angle which is defined such that $S_{11} = e^{2i\delta_{S_1^3}} \cos 2\epsilon_1$. The D_1^3 elastic phase shifts are presented in the fig.8 and will be discussed below together with the rest of D-waves. The agreement is remarkably good for the S_1^3 phase shifts and promising for the ϵ_1 parameter, in the sense that the NNLO contributions are expected to improve the agreement with the ϵ_1 data. In the same figure we also present the resulting curves from the scheme presented in this work at NLO. So as to reduce the number of our free parameters as much as possible we impose that $\nu_2 = \nu_1$, that is quite natural if we think of the ν_i as coming from a cut-off as discussed above. This constraint together with eqs.(3.6), which fix ξ_1 and ξ_2 in terms of the ERE parameters, $a_s = 5.425$ fm and $r_0 = 1.749$ fm, implies that only γ and ν_1 remain as free parameters. We then obtain after the fit to the scattering data:

$$\gamma = 0.41 \text{ fm}^{-1}, \quad \xi_1^* = 0.33, \quad \xi_2^* = -0.06, \quad \nu_2^* = \nu_1 = 670 \text{ MeV}. \tag{3.9}$$

The resulting curves are the solid ones in fig.3. These curves lie in general somewhat closer to data than those of the pure KSW treatment of ref.[14] at NLO, particularly for cm three-momentum above 150 MeV. In addition we also consider the sensitivity of our results under a change of the subtraction constants ν_2 and ν_1 . The short-dashed curves, the one lying highest in the left panel, correspond to fixing $\nu_2 = \nu_1 = 800$ MeV and then γ is fitted with the result $\gamma = 0.41 \text{ fm}^{-1}$ with $\xi_1^* = 0.32$ and $\xi_2^* = -0.02$. Analogously, the lowest lying curve in the S_1^3 phase shifts, the dashed ones, corresponds to taking $\nu_2 = \nu_1 = 200$ MeV and then $\gamma = 0.42 \text{ fm}^{-1}$, $\xi_1^* = 0.44$ and $\xi_2^* = 0.06$. Taking into account the lists of values for ν given in table 1 as a function of an hypothetical cut-off, it is clear that a variation of the ν 's from 200 MeV to 900 MeV, with the best fit at $\nu_2 = \nu_1 = 670$ MeV, can be recast as a large variation of Q , from around 300 MeV up to 1.6 GeV. It is also remarkable the constancy of the value of γ around 0.41 fm^{-1} .

Now we come to the NNLO order results both at the perturbative level of ref.[14] as well as from our scheme. As before, we consider first the pure KSW analysis [14]. The value of γ is the same as the one at NLO eq.(3.8), since the pole in the perturbative treatment comes only from A_{-1} , the leading contribution. Similarly as at NLO, the number of free counterterms can be reduced by requiring the absence of double and triple poles that appear in the NNLO KSW amplitudes. As a result, ξ_2 and ξ_3 are expressed in terms of ξ_1 and ξ_4 . Thus the free counterterms

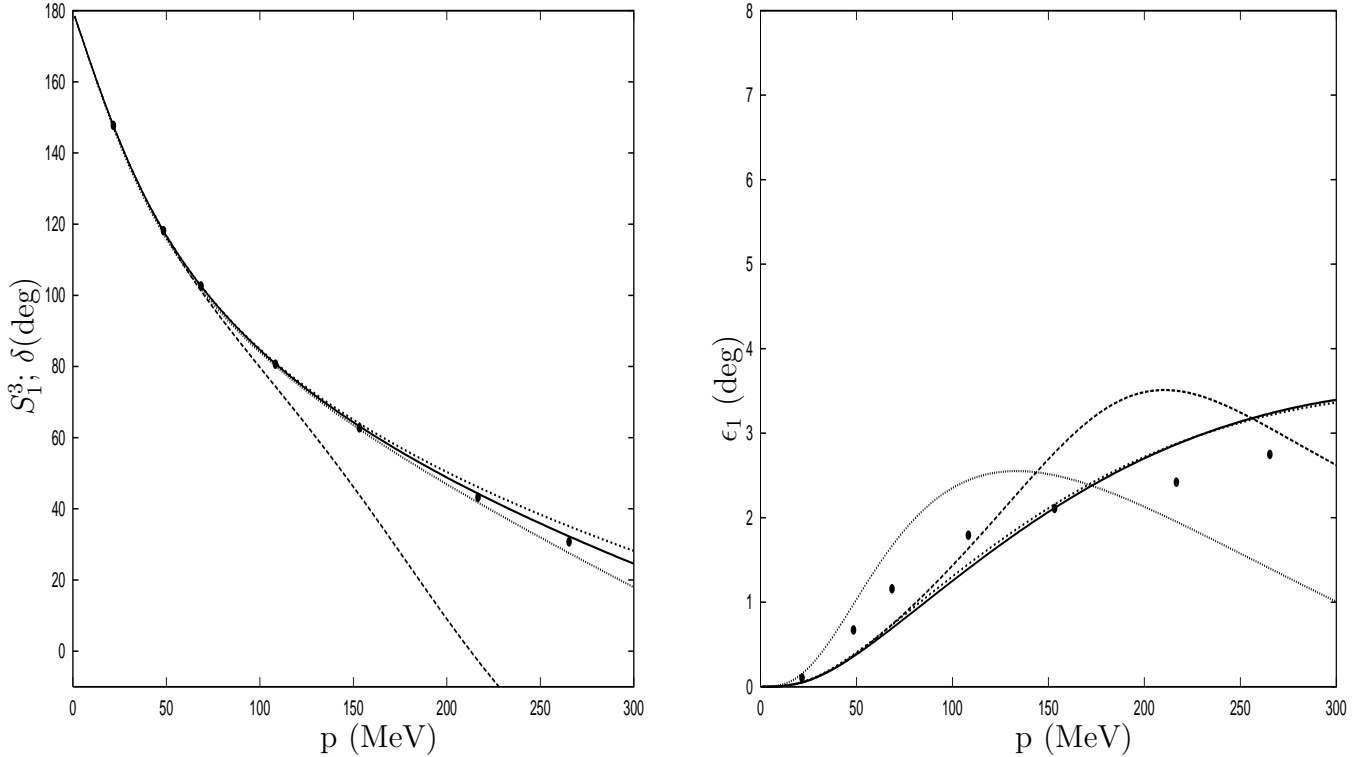


Figure 3: Phase shifts for the S_1^3 channel and mixing angle ϵ_1 . The dotted lines are the NLO KSW results [14]. The solid lines are the results from our approach corresponding to the fit of eq.(3.9). In the short-dashed lines the subtraction constants ν_1 and ν_2 are fixed at 800 MeV. The dashed lines correspond to fixing ν_1 and ν_2 at 200 MeV. The data come from the Nijmegen partial wave analysis, ref.[24].

present in ref.[14] are finally ξ_1, ξ_4, ξ_5 and ξ_6 , which are fitted to the S-wave scattering data, at this order the D_1^3 elastic phase shifts are free of any NNLO counterterm. The counterterm ξ_6 does not affect the elastic S_1^3 phase shifts and only influences the ϵ_1 mixing angle. The dotted lines in fig.4 correspond to the pure KSW treatment with the set of values [14]:

$$\gamma^* = 0.23 \text{ fm}^{-1}, \quad \xi_1 = 0.432, \quad \xi_2^* = -0.0818, \quad \xi_3^* = 0.165, \quad \xi_4 = 0.399, \quad \xi_5 = 0.26, \quad (3.10)$$

by fitting the elastic S_1^3 phase shifts. The counterterms with a star are not taken as free parameters in the fit as usual. The resulting phase shifts are shown in the left panel of fig.4 by the dotted line. In the second entry of ref.[14] only the mixing angle ϵ_1 was considered and a fit was performed exclusively to the ϵ_1 data from ref.[24], without considering the S_1^3 phase shifts. The new set of values are:

$$\gamma^* = 0.23 \text{ fm}^{-1}, \quad \xi_1 = 0.235, \quad \xi_2^* = -0.104, \quad \xi_6 = 0.385. \quad (3.11)$$

The resulting S_1^3 phase shifts are much worse than those from the set of eq.(3.10). Thus we only show the curves with the values of eq.(3.10) and then we determine ξ_6 by performing a fit to the ϵ_1 data with the rest of counterterms fixed at the values of eq.(3.10). We obtain then $\xi_6 = 0.50$ and the resulting curve for ϵ_1 is the dotted line shown in the right panel of fig.4. As it is well known from the results of ref.[14], the NNLO results are worse than those at NLO already for $p \gtrsim 100$

MeV, despite the pion fields being explicitly included in the effective field theory. The results shown in ref.[14] from the set of values of eq.(3.11) give rise to the same divergent behavior as that indicated by the dotted lines of fig.4. It was also noted in ref.[14] that this bad behavior was due to large corrections from the twice iterated one pion exchange diagrams which are enhanced by large numerical factors. In our power counting the input kernel, \mathcal{R} , is infinitely iterated and with it the pion exchange as any other contribution.

We now consider the results we obtain from our novel non-perturbative approach at NNLO order in the expansion of \mathcal{R} . We follow the same treatment for the counterterms as explained in the S_0^1 case, so that ξ_1, ξ_2 and ξ_3, ξ_4 are fixed in terms of the ERE parameters at NLO eq.(3.6) and at NNLO eq.(3.7), respectively. Performing a fit to the scattering data, S_1^3 phase shifts and ϵ_1 mixing angle, up to $p \leq 300$ MeV, the values we obtain are:

$$\begin{aligned} \gamma = 0.37 \text{ fm}^{-1}, \quad \xi_1^* = 0.44, \quad \xi_2^* = 0.01, \quad \xi_3^* = 0.05, \quad \xi_4^* = 0.04, \quad \xi_5 = 0.19, \quad \xi_6 = 0.58, \\ \nu_1 = 190 \text{ MeV}, \quad \nu_2 = 620 \text{ MeV}. \end{aligned} \tag{3.12}$$

The results of this fit are presented in the left and right panels of fig.4 by the solid lines. As we see the agreement with data is remarkably good. We now show the sensitivity of the results under changes of the subtraction constants ν_1 and ν_2 . For that, we first impose the constraint $\nu_2 = \nu_1$ as in the NLO case, and perform the fit. The fitted parameters are:

$$\begin{aligned} \gamma = 0.41 \text{ fm}^{-1}, \quad \xi_1^* = 0.34, \quad \xi_2^* = 0.00, \quad \xi_3^* = 0.06, \quad \xi_4^* = 0.16, \quad \xi_5 = 0.25, \quad \xi_6 = 0.51, \\ \nu_1 = 500 \text{ MeV}, \quad \nu_2^* = 500 \text{ MeV}. \end{aligned} \tag{3.13}$$

the results are shown in fig.4 by the dashed lines. They are quite similar to those of the fit of eq.(3.12) and essentially identical for the ϵ_1 mixing angle. Let us note that ν_1 has changed very appreciably with respect to eq.(3.12) and the fit continues being rather acceptable. Finally, in order to have as well a large variation of ν_2 from the value given in eq.(3.12), we fix $\nu_1 = 600$ MeV and $\nu_2 = 200$ MeV and fit γ, ξ_5, ξ_6 . The resulting values are:

$$\begin{aligned} \gamma = 0.55 \text{ fm}^{-1}, \quad \xi_1^* = 0.33, \quad \xi_2^* = 0.10, \quad \xi_3^* = -0.19, \quad \xi_4^* = -0.11, \quad \xi_5 = 0.20, \quad \xi_6 = 0.57, \\ \nu_1^* = 600 \text{ MeV}, \quad \nu_2^* = 200 \text{ MeV}. \end{aligned} \tag{3.14}$$

The results correspond to the short dashed lines. The S_1^3 phase shifts are very similar to those of the best fit of eq.(3.12) although the ϵ_1 mixing angle curve is more different than that obtained from the fit with $\nu_2 = \nu_1$, eq.(3.13). Thus, we see that the dependence on the subtraction constants ν_1 and ν_2 is rather mild and can be reabsorbed to a large extent in new values of the KSW counterterms, γ and ξ_i .

In the KSW approach, when solving the renormalization group equations one has [14],

$$\xi_5 = \rho \frac{m_\pi^2 M}{4\pi} \tag{3.15}$$

and since ρ is order p^0 , given by Λ_{NN} , then ξ_5 is formally a quantity of order p^2 . Hence, within the KSW scheme its contributions to the scattering amplitude are order p^2 and start at N³LO. This situation is the standard one in ref.[14] and the results from the KSW perturbative treatment with

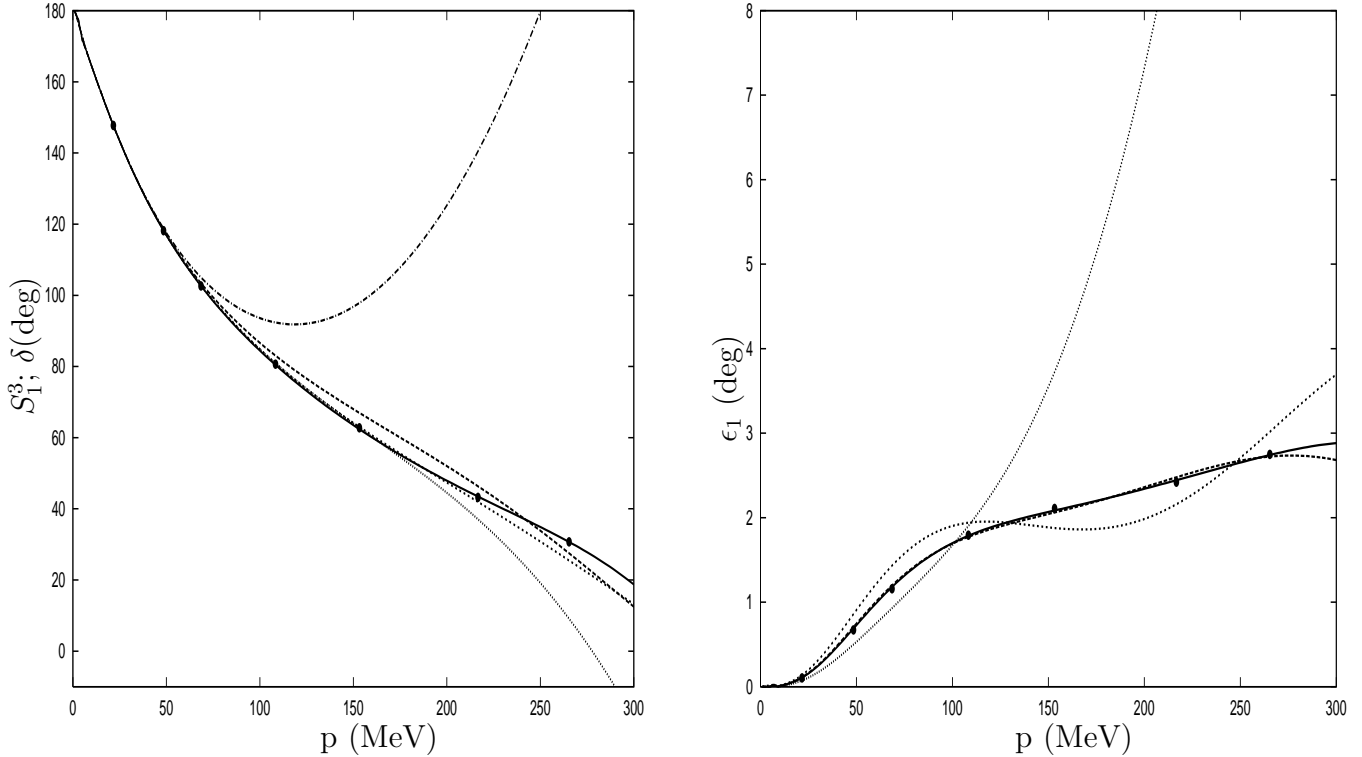


Figure 4: Phase shifts for the S_1^3 channel and mixing angle ϵ_1 . The dotted lines are the NNLO KSW results of ref.[14] with $\xi_5 \neq 0$ and the dashed-dotted line of the left panel when $\xi_5 = 0$. The solid lines correspond to the fit of eq.(3.12). The dashed ones are the fit of eq.(3.13). The short dashed lines correspond to the results of eq.(3.14). For further details see the text. The data are from the Nijmegen partial wave analysis, ref.[24].

$\xi_5 = 0$, with the rest of counterterms $\xi_1 - \xi_4$ given in eq.(3.11), correspond to the dashed-dotted line in fig.4, the one that lies above all the other ones in the left panel. We see then that the elastic S_1^3 phase shifts diverge for cm three-momenta much smaller than for the $\xi_5 \neq 0$ case but similar to those cm three-momenta where the divergence starts for the ϵ_1 mixing angle, which indeed is independent of ξ_5 at NNLO in the KSW approach.

Now, let us discuss why in our approach we should take ξ_5 as a free parameter without taking into account eq.(3.15). The point is the following. The order of the counterterms in KSW, in particular those given rise to ξ_5 , are determined by comparing with the effective range expansion in the pionless effective field theory once the power divergence subtraction (PDS) scheme is adopted [13]. This comparison is exact, even if the series are truncated, since both of them implies an expansion in powers of the cm three-momentum and the comparison is performed order by order. In this process one formally books the scattering length as order p^{-1} and the shape parameters r_n as order zero, proportional to $1/\Lambda_{NN}$. Once this is performed, those operators that enter in the Lagrangian up to some order can be determined, and then the corresponding KSW partial wave amplitudes up to the same order can be calculated as well. As we have already explained, these amplitudes are taken as the input of our approach in order to fix \mathcal{R} by the matching process

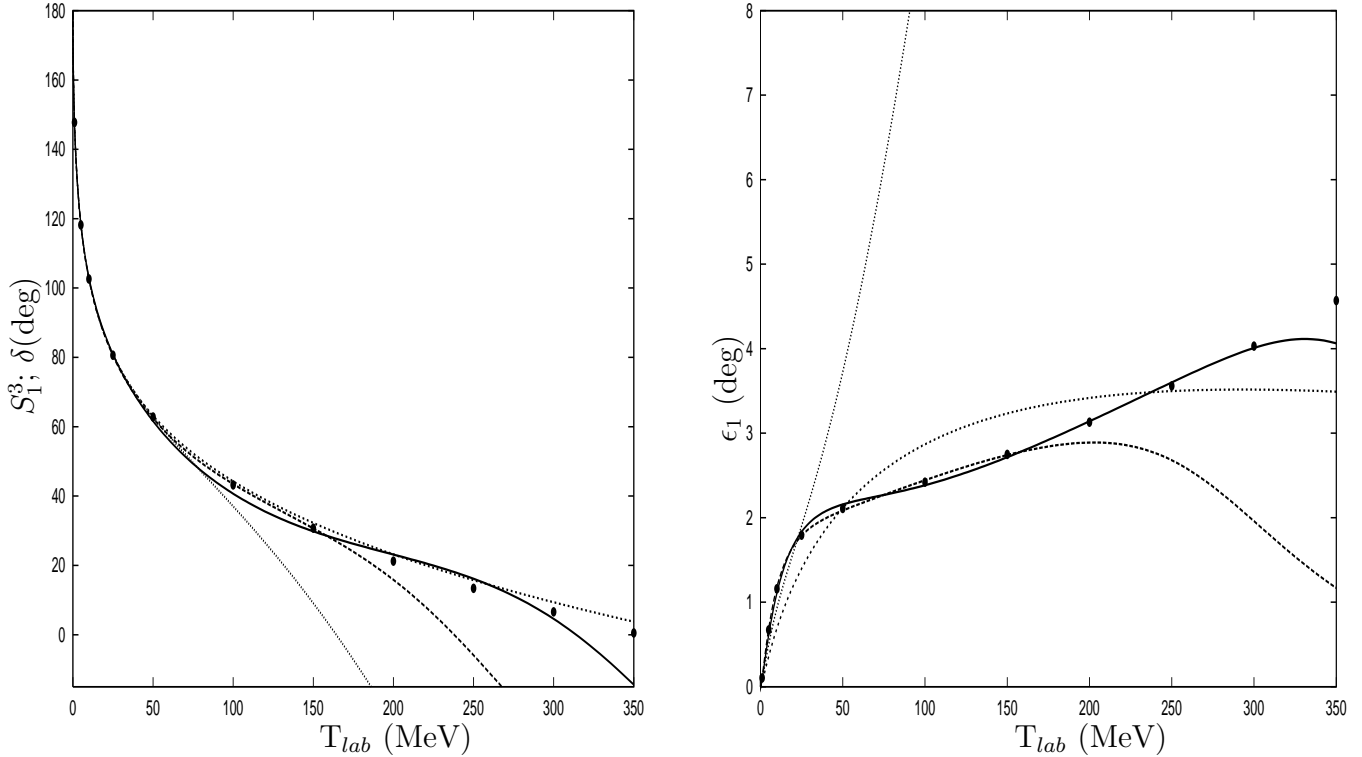


Figure 5: Phase shifts for the S_1^3 channel and mixing angle ϵ_1 . The dotted lines are the NNLO KSW result [14] with $\xi_5 \neq 0$. The short dashed lines represent the NLO results from eq.(3.9). The dashed lines are the NNLO fit to data for $p \leq 300$ MeV given in eq.(3.12). The solid lines are the new fit of eq.(3.16) for $p \leq 400$ MeV. The data correspond to the Nijmegen partial wave analysis, ref.[24].

outlined above in sec.2. In the pure KSW treatment one requires the amplitudes being independent under changes of the subtraction point so that the renormalization group equations (RGE) follow for the different local counterterms. In practice, even when pions are removed and only local operators remain, this guarantees that the scattering partial wave is subtraction point independent only perturbatively, in the sense that this only happens when the Schrödinger equation is solved perturbatively.^{#6} But this is precisely the point we want to avoid in our formalism so as to take care properly of the large $2M/p$ factors that appear from the two nucleon intermediate states in the unitarity bubbles. At this point our formalism is an hybrid between that of Weinberg [5] and the KSW formalism [13]. On the one hand, we perform an expansion of an interacting kernel \mathcal{R} as in ref.[5] but on the other we do that by considering directly the scattering amplitudes as in ref.[13]. Indeed, there is a residual dependence in our amplitudes on the subtraction constant ν , expected to correspond to higher order operators in the KSW Lagrangian, similarly as in the Weinberg approach where there is cut-off dependence that is expected to become softer as the order of the calculation increases, as also occurs in our case as discussed above. To sum up, our scheme makes use of the KSW power counting in order to obtain the Lagrangian, employs Feynman diagrams

^{#6}This acquires a clear meaning if one thinks of the pionless effective field theory, where to solve the Schrödinger equation is a trivial task.

to calculate from this Lagrangian the KSW amplitudes at some order (where the order of any combination of counterterms is determined directly from the ones of the original counterterms in the Lagrangian, without making use of perturbative RGE arguments). Then, these amplitudes are matched with the general expression of eq.(2.5) so that the interacting kernel \mathcal{R} is determined. Thus, as a result, one ends with partial wave amplitudes with the unitarity bubbles resummed as in Weinberg's scheme but in an analytical way based on unitarity and analyticity.

Encouraged by the rather good fits obtained from our approach up to $p \lesssim 300$ MeV as depicted in figs.3 and 4, we now show in fig.5 our results for higher energies, namely for $T_{lab} \lesssim 350$ MeV, as similarly shown in the studies of nucleon-nucleon scattering within the Weinberg approach in ref.[12]. Let us note that for $p = 300$ MeV one has $T_{lab} \simeq 190$ MeV. We present in fig.5 several lines. The dashed lines correspond to the solid ones of fig.4, with the parameters given in eq.(3.12). We see, as already shown in fig.4, that the agreement with data for $T_{lab} \lesssim 190$ MeV is very good but from $T_{lab} = 200$ MeV starts deviating from data. The dotted lines are the NNLO KSW results from ref.[14] with $\xi_5 \neq 0$, already presented in fig.4 with the same type of line. We also show with the short-dashed lines our NLO results given in eq.(3.9) with only two free parameters in the fit. We see that they follow closely the trend of the S_1^3 phase shifts in all the energy interval although the agreement is not so good for the ϵ_1 , similarly as also happens in the KSW treatment at NLO. Finally by the solid line we present a new fit up to $p \leq 400$ MeV, where ξ_1 and ξ_2 are fitted, instead of begin fixed by the ERE at NLO, eqs.(3.6). On the other hand, ξ_3 and ξ_4 continue to be given in terms of ξ_1 , ξ_2 and γ from eqs.(3.7). The resulting parameters are:

$$\begin{aligned} \gamma = 0.51 \text{ fm}^{-1} , \quad \xi_1 = 0.27 , \quad \xi_2 = 0.06 , \quad \xi_3^* = -0.10 , \quad \xi_4^* = -0.05 , \quad \xi_5 = 0.17 , \quad \xi_6 = 0.46 , \\ \nu_1 = 180 \text{ MeV} , \quad \nu_2 = 560 \text{ MeV} . \end{aligned} \tag{3.16}$$

The reproduction of the data is quite good, specially for the mixing angle ϵ_1 . Nevertheless, we observe some deviation from data in the low energy region around $T_{lab} \simeq 100$ MeV ($p \simeq 215$ MeV) which does not appear in the other fits obtained by fitting data only up to $p = 300$ MeV or $T_{lab} \lesssim 190$ MeV, that is for lower energies. This can be interpreted as an indication that we are forcing too much the capability of our approach accordingly with an estimated Λ_{NN} around 400 MeV. This is also supported by the divergence of the fit of eq.(3.12) for T_{lab} above 200 MeV, solid lines in fig.4 and dashed ones in fig.5, as well as from the results shown in fig.6 which are discussed in the next paragraph. In this sense the fit given in eq.(3.16) is just a way to fit data up to rather high energies. Nonetheless, it is reassuring that the values of the parameters, although there are now two free parameters more, are very similar to those obtained above for lower energies, e.g. in eq.(3.12).

We also show in fig.6 the absolute values $|\mathcal{R}^{NLO}|$ and $|\mathcal{R}^{NNLO}|$ for the S_0^1 channel (solid lines) and the same, although divided by four to keep the lines on the same scale, for the matrix element $|R_{11}|$ of the S_1^3 channel. The thick lines refer to the NNLO calculations and the thin ones to NLO. The convergence properties are quite good in a broad range of the center of mass three momentum p , with strong divergences for p around $\Lambda_{NN} \simeq 400$ MeV. This scale is the one expected for the KSW EFT [13], although in the end this EFT does not converge in the triplet channels for $p \gtrsim 100$ MeV, as already discussed. We see that within our scheme, at the same time that we keep the KSW power counting, we are able to fulfill these expectations. This is the main aim of the present investigation.

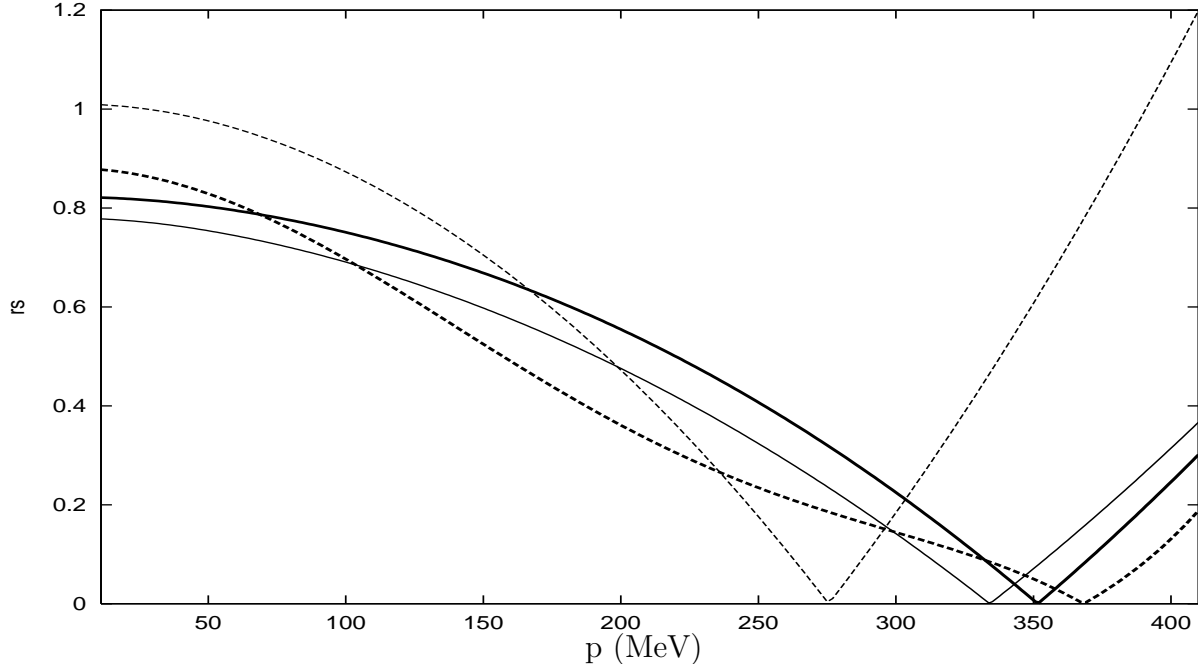


Figure 6: $|\mathcal{R}^{NLO}|$ (thin solid line), $|\mathcal{R}^{NNLO}|$ (thick solid line) for the S_0^1 channel and $|R_{11}^{NLO}/4|$ (thin dashed line) and $|R_{11}^{NNLO}/4|$ (thick dashed line) for the S_1^3 channel, as a function of the cm three-momentum.

3.3 P , D , F_2^3 and G_3^3 partial waves

Up to NNLO in the KSW approach, order p , the physics included in the description of partial waves higher than S waves, except for the mixing between the $S_1^3 - D_1^3$ ones, consists only of the one pion exchange, order p^0 , and the reducible part of the twice iterated one pion exchange, order p . While the former contribution constitutes the LO one of the Weinberg's scheme [6, 12], the latter is generated by solving the Lippmann-Schwinger equation. Hence, the NNLO results in the KSW approach are included in the leading ones of Weinberg's scheme. It is clear then that we are neglecting important contributions for the higher partial waves, particularly for the P and D waves, since from the results of the Weinberg's approach we know that two pion exchange irreducible diagrams, counterterms for the P -waves at order p^2 , as well as the πN counterterms (which are saturated to a large extent by the Δ isobar) are important contributions that would rise in higher order calculation within the KSW, beyond NNLO. Hence a full N^3 LO calculation from the KSW Lagrangian should be pursued and then used within our approach to offer a more complete study of these higher partial waves. For the F and G waves and mixing parameters ϵ_2 and ϵ_3 , pion exchange dominates and the aforementioned extra contributions are not so important, see e.g. [25]. This is also clear from our results given in figs. 7 and 8. At the order we are working in these partial waves there are no counterterms and the only free parameters are the subtraction constants ν 's, one for each partial wave. In most of the channels, they take arbitrarily large or negative values, that is, any value with modulus typically above $\Lambda_{\chi p T} \simeq 0.7 - 1$ GeV gives essentially the same results. Our curves are indeed quite similar to those obtained in the Weinberg's approach at LO,

see [12]. Our results at NNLO, solid lines, improve those of the NLO, dashed lines, except for the D_1^3 where, though the NNLO is better at low T_{lab} , they depart from data more than the NLO ones for higher energies. They also improve the results from the pure KSW amplitudes, dotted lines, although in these cases, as expected, the resummation effects are not so important as in the S-waves.

Since most of the subtraction constants ν for the analyzed P , D , F and G waves take arbitrarily large absolute values we would like to show that in the limit when $|\nu| \rightarrow \infty$ our approach reduces to the Inverse Amplitude Method [22]. This method would consist of expanding the inverse of a partial wave, following in our present problem the KSW power counting, and then calculate the partial wave by inverting exactly the previous expansion. For instance, we have given in eq.(2.15) the expansion of the inverse of the elastic S_0^1 partial wave within the KSW power counting (in ref.[22] one uses for meson-meson scattering the standard chiral perturbation theory counting and for pion-nucleon processes the chiral perturbation theory counting is supplied with the heavy baryon one). Then the inverse amplitude method would imply:

$$T_{S_0^1, S_0^1} = \left[\left(\frac{1}{A_{-1}} \right) - \left(\frac{A_0}{A_{-1}^2} \right) + \left(\frac{A_0^2 - A_1 A_{-1}}{A_{-1}^3} \right) \right]^{-1}. \quad (3.17)$$

Its generalization to coupled channels is straightforward by making use of a matrix notation. For example in the $S_1^3 - D_1^3$ coupled channels one should just invert exactly the matrix $(A_{S_1^3 - D_1^3}^{KSW})^{-1}$ whose matrix elements are given in eqs.(2.25), and so on for any other partial waves. This kind of results are also usually referred as Padé resummations.

Let us see that our formalism reduces to the inverse amplitude method when $|\nu| \rightarrow \infty$. Consider first the elastic case. Then, the contribution of order p^i in the KSW power counting, from the expansion of $1/\mathcal{R} + g$ in eq.(2.5), has one piece involving the R_i component of \mathcal{R} . Isolating R_i one has:

$$R_i = -R_0^2 [(1/A)_i + g_i] + \dots, \quad (3.18)$$

where g_i is now the contribution of the g function of order p^i and $(1/A)_i$ is that of the inverse of the KSW partial wave. Since R_0 scales as $1/\nu$, see eq.(2.18) for the case of large scattering lengths and (2.31) for the case of natural ones, then R_i has a contribution scaling as $1/\nu^2$. This is the only contribution for $i = 1$ and then R_1 scales as $1/\nu^2$. Let us demonstrate by induction that each R_i with $i \geq 1$ scales as $1/\nu^2$, while R_0 scales only as $1/\nu$. To show that, let us consider the dots which indicate other terms from the expansion of $1/\mathcal{R}$ involving R_m with $1 \leq m \leq i - 1$. We can write these contributions as:

$$\sum_{m=1}^{i-1} C_{k_1 k_2 \dots k_m}^{a_1 a_2 \dots a_m} \frac{R_{k_1}^{a_1} R_{k_2}^{a_2} \dots R_{k_m}^{a_m}}{R_0^{a_1 + a_2 + \dots + a_m - 1}}, \quad (3.19)$$

where k_p ($1 \leq p \leq i - 1$) indicates the order of the corresponding factor R_{k_p} , in addition all the k_p are different from each other and fulfill $a_1 k_1 + a_2 k_2 + \dots + a_m k_m = i$. Because each of the R_{k_p} in eq.(3.19) scales at least as $1/\nu^2$ one can count easily the dominant power of ν from eq.(3.19) when $|\nu| \rightarrow \infty$. One simply has:

$$\frac{\nu^{a_1 + a_2 + \dots + a_m - 1}}{\nu^{2(a_1 + a_2 + \dots + a_m)}} = \frac{1}{\nu^{a_1 + a_2 + \dots + a_m + 1}}. \quad (3.20)$$

But the sum $a_1 + a_2 + \dots + a_n + 1 \geq 3$. To show this, let us consider first those terms in the sum of eq.(3.19) with all the factors the same and equal to R_{k_1} . It follows then that $a_1 \geq 2$ since $1 \leq k_1 \leq i - 1$. The rest of terms will have at least two different factors, then there must be two a 's, let us say a_1 and a_2 , different from zero and every one ≥ 1 . Then the scaling of R_i in ν when $|\nu| \rightarrow \infty$ is dominated the one from eq.(3.18) and goes like $1/\nu^2$.

Let us consider the expansion of $1/\mathcal{R} + g$ in eq.(2.5) in powers of $1/\nu$ in the limit $|\nu| \rightarrow \infty$ with \mathcal{R} determined up to order p^n in the KSW counting. We also write for g only the sum $\sum_{k=0}^n g_k$ since higher order terms are just relativistic corrections and numerically are negligible:

$$2T_{L_J^{2S+1}, L_J^{2S+1}} = - \left(\frac{1}{R_0 + \sum_{m=1}^n R_m} + \sum_{k=0}^n g_k \right)^{-1} = - \left(\frac{1}{R_0} - \sum_{m=1}^n \frac{R_m}{R_0^2} + \mathcal{O}(\nu^{-1}) + \sum_{k=0}^n g_k \right)^{-1}. \quad (3.21)$$

Where we neglect the $\mathcal{O}(\nu^{-1})$ terms compared to those explicitly shown in the equation above which are $\mathcal{O}(\nu^0)$ and are the only ones that survive in the limit $|\nu| \rightarrow \infty$. Thus, as a result of the matching process detailed in sec.2 to obtain the R_i functions that we apply now for $|\nu| \rightarrow \infty$, one has between the brackets of eq.(3.21) the expansion of the inverse of the KSW amplitude up to order p^n . So that the resulting $T_{L_J^{2S+1}, L_J^{2S+1}}$ partial wave from eq.(2.5) for $|\nu| \rightarrow \infty$ is the one given by the inverse amplitude method eq.(3.17). For finite ν 's this is no longer the case. The neglected terms of order ν^{-1} and higher in eq.(3.21) guarantee the matching with the expansion of the inverse the KSW amplitudes up to order p^n and also give rise to higher order terms beyond those considered in the matching process. It is only necessary a little thought to extend this discussion for the elastic case to the coupled channel one by making use of a matrix language.

4 Conclusions

We have established a new analytic expansion in order to treat systematically nucleon-nucleon interactions. Analyticity and unitarity properties of the inverse of a partial wave amplitude are used to resum the unitarity bubbles in terms of an on-shell interacting kernel \mathcal{R} and the unitarity loop function g . The former is determined by performing an expansion with the KSW power counting of the aforementioned general expression for a partial wave and by matching this expansion with that of the inverses of the pure KSW amplitudes up to a definite order. In practice we have performed this matching with NLO and NNLO KSW amplitudes [13, 14]. As a result, a hybrid scheme emerges that treats pions non-perturbatively but in harmony with the KSW power counting, and that restores the expected range of convergence of the KSW EFT about $\Lambda_{NN} = 400$ MeV. It reminds also the Weinberg's approach [5] in that a perturbative expansion is performed for an interacting kernel instead of making it directly to the partial waves. In our case this interacting kernel is \mathcal{R} while in Weinberg's approach is the potential, V . However, it is worth stressing that while \mathcal{R} is on-shell, V is off-shell and this is an important point that allows our formalism to be purely analytic and fairly more simple than that of ref.[5]. It is also important to remark that for the S-waves we have achieved a very good agreement with data, both for the phase shifts as well as for the mixing angle ϵ_1 , up to the opening of the $NN\pi$ threshold.

Further applications of the present scheme should be pursued, particularly to three body problem where the disposal of analytical methods in the two-nucleon sector is well worth [28] and

furthermore a KSW N³LO calculation should also be performed within our scheme particularly for a more complete study of the P and D partial waves. Finally, another issue is to extend this knowledge of the nucleon-nucleon interactions in vacuum to nuclear matter [29, 30].

Acknowledgments

I would like to thank E. Epelbaum for interesting discussions that we held in Jülich on nucleon-nucleon interactions. I am also grateful to the Benasque Center for Science, where part of this work was done, for its support and enjoyable atmosphere. This work is partially supported by the DGICYT project FPA2002-03265.

References

- [1] S. Weinberg, *Physica* **A96**, 327 (1979).
- [2] J. Gasser and H. Leutwyler, *Ann. Phys. (N.Y.)* **158**, 142 (1984).
- [3] U.-G. Meißner, *Rep. Prog. Phys.* **56**, 903 (1993);
G. Ecker, *Prog. Part. Nucl. Phys.* **35**, 1 (1995);
A. Pich, *Rep. Prog. Phys.* **58**, 563 (1995);
H. Leutwyler, *Encyclopedia of Analytic QCD*, edited by M. Shifman, World Scientific; hep-ph/0008124
- [4] U.-G. Meißner, *Encyclopedia of Analytic QCD*, edited by M. Shifman, World Scientific; hep-ph/0007092.
- [5] S. Weinberg, *Phys. Lett.* **B251**, 288 (1990); *Nucl. Phys.* **B363**, 3 (1991).
- [6] C. Ordóñez, U. van Kolck, *Phys. Lett.* **B291**, 459 (1992);
C. Ordóñez, L. Ray and U. van Kolck, *Phys. Rev. Lett.* **72**, 1982 (1994); *Phys. Rev.* **C53**, 2086 (1996);
U. van Kolck, *Phys. Rev.* **C49**, 2932 (1994).
- [7] T.S. Park, D.P. Min and M. Rho, *Phys. Rev. Lett.* **74**, 4153 (1995); *Nucl. Phys.* **A596**, 515 (1996).
- [8] D.B. Kaplan, M.J. Savage and M.B. Wise, *Nucl. Phys.* **B478**, 629 (1996).
- [9] D. Eiras and J. Soto, nucl-th/0107009.
- [10] J. Nieves, nucl-th/0301080.
- [11] S.R. Beane, P.F. Bedaque, W.C. Haxton, D.R. Phillips and M.J. Savage, *Encyclopedia of Analytic QCD*, edited by M. Shifman, World Scientific; hep-ph/0008064.
- [12] E. Epelbaum, W. Glöckle, U.-G. Meißner, *Nucl. Phys.* **A637**, 107 (1998); *Nucl. Phys.* **A671**, 295 (2000).
- [13] D.B. Kaplan, M.J. Savage and M.B. Wise, *Phys. Lett.* **B424**, 390 (1998); *Nucl. Phys.* **B534**, 329 (1998).

- [14] S. Fleming, T. Mehen and I. Stewart, Nucl. Phys. **A677**, 313 (2000); Phys. Rev. **C61**, 044005 (2000).
- [15] T.D. Cohen and J.M. Hansen, Phys. Rev. **C59**, 13 (1999); Phys. Rev. **C59**, 3047 (1999).
- [16] M. Lutz, Nucl. Phys. **A677**, 241 (2000).
- [17] G.F. Chew and S. Mandelstam, Phys. Rev. **119**, 467 (1960).
- [18] J.A. Oller and E. Oset, Phys. Rev. **D60**, 074023 (1999);
J.A. Oller, Phys. Lett. **B477**, 187 (2000);
M. Jamin, J.A. Oller and A. Pich, Nucl. Phys. **B587**, 331 (2000); Nucl. Phys. **B622**, 279 (2002); Eur. Phys. J. **C24**, 237 (2002).
- [19] J.A. Oller and E. Oset, Nucl. Phys. **A620**, 438 (1997), (E)-ibid **A652**, 407 (1999).
For a general introduction and discussion see J.A. Oller, Invited talk at YITP Workshop on Possible Existence on the Sigma Meson and its Implications to Hadron Physics, hep-ph/0007349.
- [20] U.-G. Meißner and J.A. Oller, Nucl. Phys. **A673**, 311 (2000).
- [21] J.A. Oller, U.-G. Meißner, Phys. Lett. **B500**, 263 (2001); Phys. Rev. **D64**, 014006 (2001).
- [22] A. Dobado, M.J. Herrero and T.N. Truong, Phys. Lett. **B235**, 134 (1990).
A. Dobado and J.R. Peláez, Phys. Rev. **D56**, 3057 (1997).
T. Hannah, Phys. Rev. **D55**, 5613 (1997).
J.A. Oller, E. Oset and J.R. Peláez, Phys. Rev. Lett. **80**, 3452 (1998); Phys. Rev. **D59**, 074001 (1999), (E)-ibid **D60**, 099906 (1999).
F. Guerrero and J.A. Oller, Nucl. Phys. **B537**, 459 (1999).
A. Gómez Nicola, J. Nieves, J. R. Peláez and E. Ruiz Arriola, Phys. Lett. **B486**, 77 (2000).
A. Gómez Nicola and J.R. Peláez, Phys. Rev. **D65**, 054009 (2002).
- [23] H.A. Bethe, Phys. Rev. **76**, 38 (1949).
H.A. Bethe, C. Longmire, Phys. Rev. **77**, 647 (1950).
- [24] V.G.J. Stoks, R.A.M. Klomp, C.P.F. Terheggen and J.J. de Swart, Phys. Rev. **C49**, 2950 (1994).
- [25] N. Kaiser, R. Brockmann and W. Weise, Nucl. Phys. **A625**, 758 (1997);
N. Kaiser Phys. Rev. **C65**, 017001 (2002).
- [26] I-W. Chen, G. Rupak, M.J. Savage, Nucl. Phys. **A653**, 386 (1999).
- [27] L. Castillejo, R.H. Dalitz and F.J. Dyson, Phys. Rev. **101**, 453.
- [28] P.F. Bedaque and H.W. Griesshammer, Nucl. Phys. **A671**, 357 (2000).
- [29] J.A. Oller, Phys. Rev. **C65**, 025204 (2002).
- [30] U.-G. Meißner, J.A. Oller and A. Wirzba, Ann. Phys. **297**, 27 (2002).

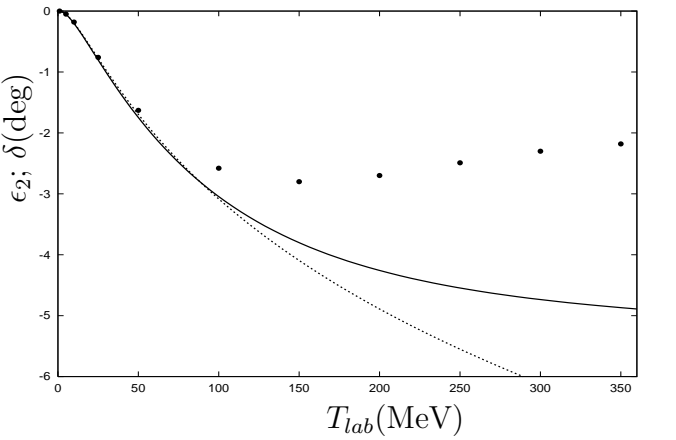
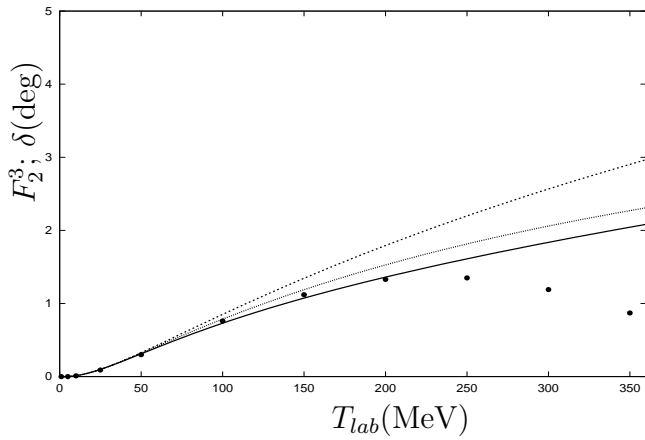
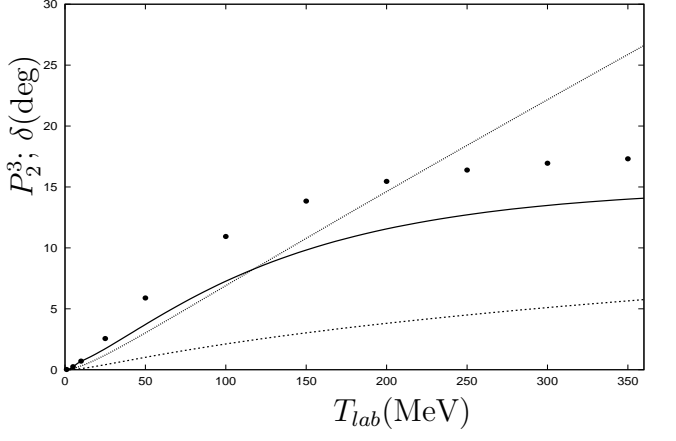
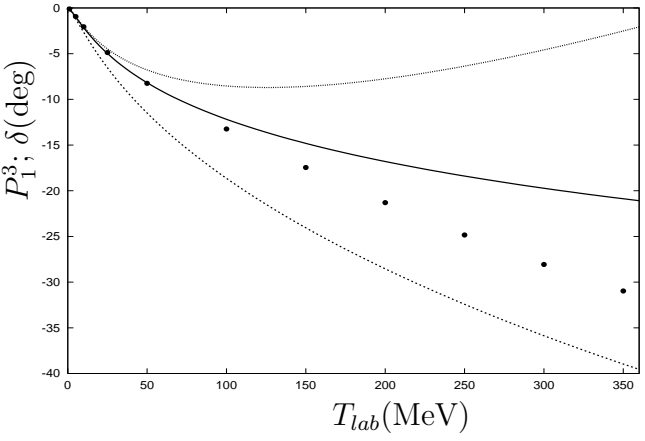
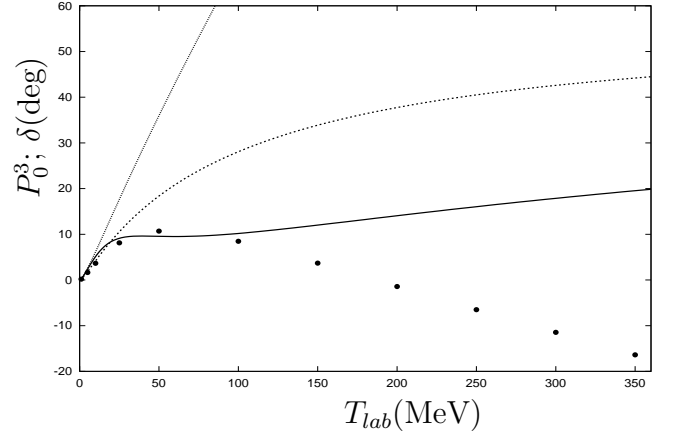
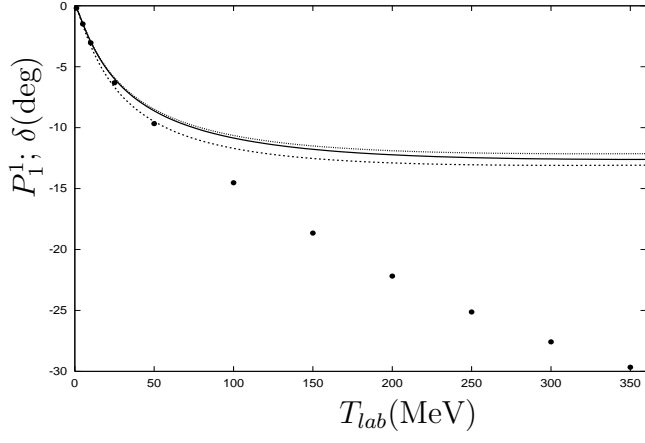


Figure 7: Phase shifts for the P_1^1 , P_0^3 , P_1^3 , P_2^3 , F_2^3 and ϵ_2 from left to right and top to bottom, respectively. The dotted line, when present, is the NNLO KSW result [14]. The dashed line represents the NLO results from eq.(2.5). The solid lines are the NNLO results. The data correspond to the Nijmegen partial wave analysis, ref.[24].

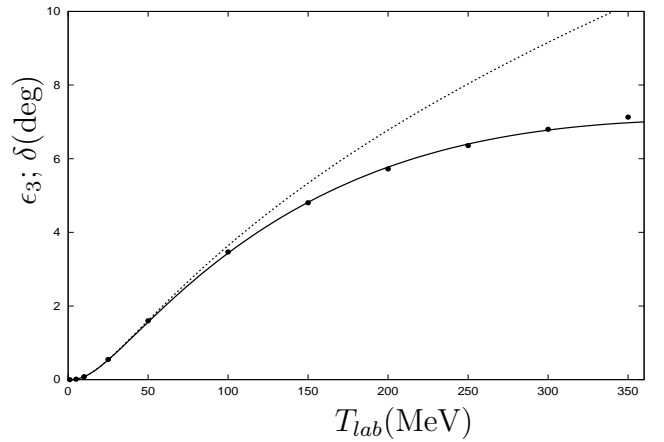
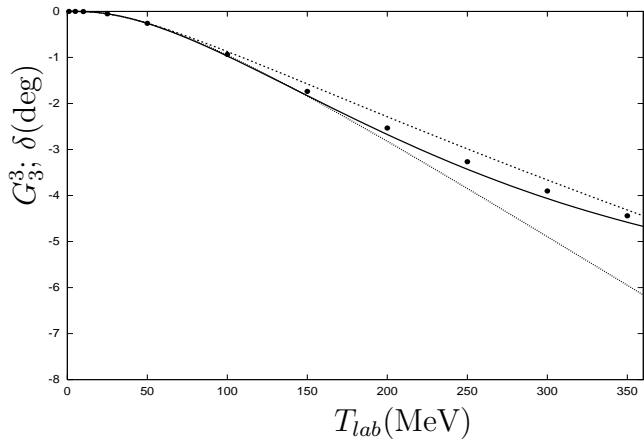
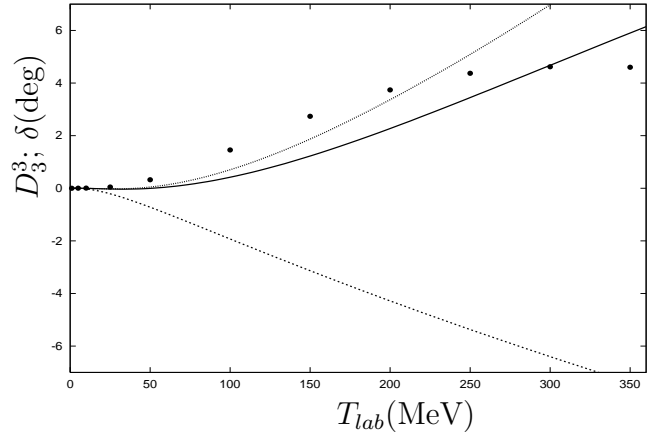
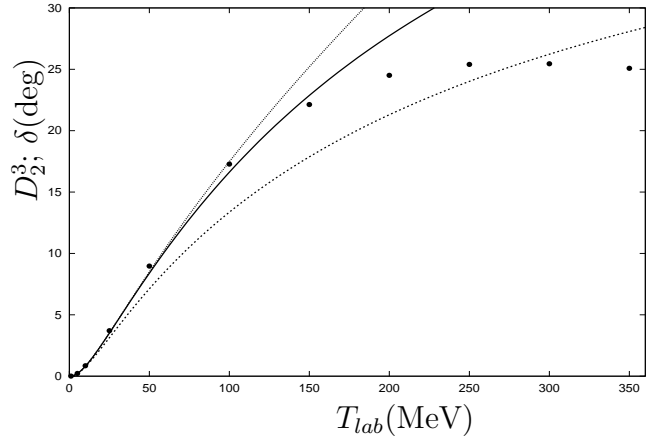
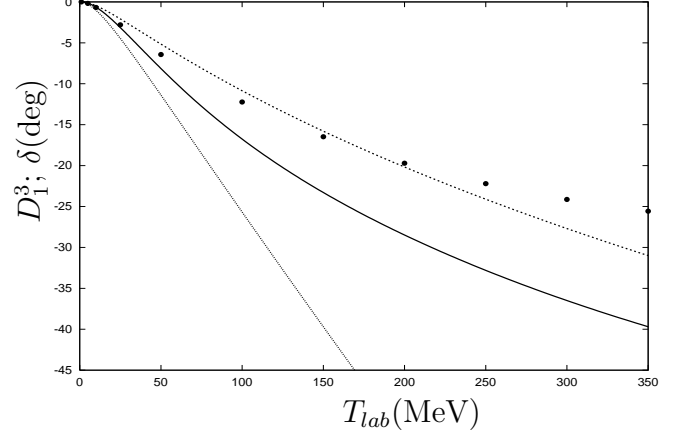
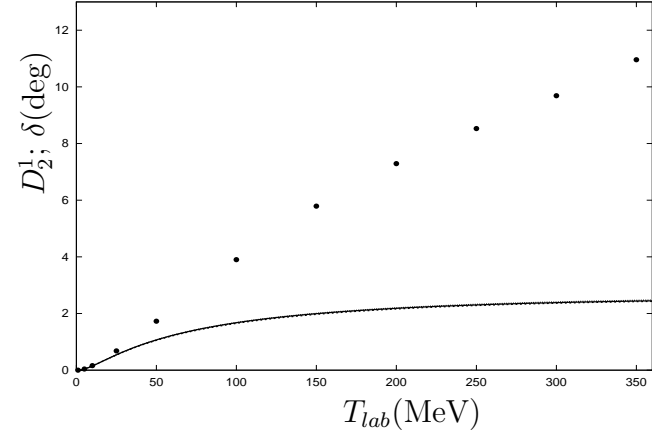


Figure 8: Phase shifts for the D_2^1 , D_1^3 , D_2^3 , D_3^3 , G_3^3 and ϵ_3 from left to right and top to bottom, respectively. The dotted line, when present, is the NNLO KSW result [14]. The dashed line represents the NLO results from eq.(2.5). The solid lines are the NNLO results. The data correspond to the Nijmegen partial wave analysis, ref.[24].